Evaluation of qPCR assays for detecting *Mycobacterium abscessus* Complex in cell-free DNA from Serum of people with Cystic Fibrosis

(Master of Biotechnology- BTEC9200B)
Microbiome Research Group

Name: Tharushi Ishara Pathirana

Student ID: 2298790

FAN: path0106

Supervisor: Prof. Geraint Rogers

Co-supervisor: Dr. Steven Taylor

Table of Contents

List of Figure

List of Tables

List of Abbreviations

BAL – Bronchoalveolar Lavage

CF – Cystic Fibrosis

cfDNA – Cell-free DNA

CRISPR – Clustered Regularly Interspaced Short Palindromic Repeats

CV – Coefficient of Variation

DNA – Deoxyribonucleic Acid

EDTA – Ethylenediaminetetraacetic Acid

gRNA – Guide RNA

LOD – Limit of Detection

MABC – *Mycobacterium abscessus* Complex

MAC – *Mycobacterium avium* Complex

Mam – *Mycobacterium abscessus* subsp. *massiliense*

Maa – *Mycobacterium abscessus* subsp. *abscessus*

Mab – *Mycobacterium abscessus* subsp. *bolletii*

MIQE - Minimum Information for publication of Quantitative real time PCR Experiment

NTM – Non-tuberculous Mycobacteria

PAM – Protospacer Adjacent Motif

PCR – Polymerase Chain Reaction

pwCF – People with Cystic Fibrosis

qPCR – Quantitative Polymerase Chain Reaction

R^2 – Coefficient of Determination

RGM – Rapidly Growing Mycobacteria

SGM – Slowly Growing Mycobacteria

Tm – Melting Temperature

Abstract

Background: Cystic Fibrosis (CF) is a life-threatening genetic disorder marked by chronic pulmonary infections. Among the emerging pathogens causing infections in people with CF (pwCF), *Mycobacterium abscessus* Complex (MABC) poses a significant clinical challenge due to its intrinsic multidrug resistance and its association with accelerated lung function decline, increased hospitalisations, and reduced eligibility for lung transplantation. Conventional diagnostic methods depend on respiratory sampling and culture-based techniques, which are typically invasive, slow, and exhibit limited sensitivity and specificity.

Aim: This study aimed to develop and validate a less invasive molecular assay for MABC detection that can be applied to pwCF. By employing quantitative PCR (qPCR) and CRISPR technology to circulating cell free DNA (cfDNA) extracted from plasma, this approach may allow cfDNA to act as a clinically useful sample for detection of life-threatening chronic lung infections.

Methods/Results: Primers that have been previously identified as selective for MABC were screened, using both in silico and in vitro testing. Among the 14 primers assessed, Primer set 6, which targets a 111bp region of the 23S rRNA gene, demonstrated high specificity towards certain NTM species and sufficient sensitivity to detect MABC. The qPCR assay demonstrated consistent reproducibility (CV <3%), maintaining linear standard curve ($R^2 > 0.99$) across a broad dynamic range of DNA input levels. When this primer was assessed on enzymatically fragmented DNA and mock plasma samples spiked with MABC DNA to simulate cfDNA conditions, sensitivity and standard curve efficiency remained high (86% -102%), albeit lower than when performed on unfragmented, pure MABC DNA. Overall, this primer was able to reliably detect MABC in mock cfDNA sample at a limit of detection of 19.5 – 21.94 copies/µL, per qPCR reaction, which falling within the clinically accepted threshold of 50 copies/µL.

To enhance the specificity of this assay, a CRISPR-Cas12a detection system was designed by developing a guide RNA that targets the same 23S rRNA amplicon region amplified by Primer Set 6. This system was intended to enable fluorescence-based detection only when the MABC-specific sequence is present, through collateral cleavage of a reporter molecule. However, due to time constraints, this CRISPR component was not experimentally validated in this study.

Conclusions: These findings provide evidence for the feasibility of cfDNA-based diagnostics for MABC using qPCR, with the potential for CRISPR integration to improve assay specificity and sensitivity. The qPCR assay using the Primer set 6 showed robust sensitivity, specificity with meeting clinically relevant detection thresholds. Future directions include integrating the CRISPR-Cas12a and validating the assay using plasma derived clinical samples from pwCF with MABC infection to assess its diagnostic performance under real world conditions. This approach establishes a foundation for less invasive, rapid, and accurate detection and monitoring of MABC infection, thereby supporting improved clinical management in pwCF.

Declaration

I certify that this thesis:

1. does not incorporate without acknowledgment any material previously submitted for a degree or diploma in any university
2. and the research within will not be submitted for any other future degree or diploma without the permission of Flinders University; and
3. to the best of my knowledge and belief, does not contain any material previously published or written by another person except where due reference is made in the text.

Signature - 

Date – 02.06.2025.

Acknowledgement

My sincere gratitude and heartful appreciation are hereby extended to the following who never ceased helping me until this research project. I would like to thank my Research supervisors, Professor Geraint Rogers and Dr. Steven Taylor, most sincerely for their unwavering support, motivation, and dedication over the duration of this research. Your professionalism and mentorship were of immense value to me in charting the path of this work and overcoming its challenges.

I am also truly appreciative Sarah Sims guidance throughout the project, skill in laboratory work and patient support along each phase of the experimental process have been invaluable to the completion of this research. Sarah, your scientific ability and helpful criticisms have polished my analysis methodology and expanded my horizons.

I would also like to sincerely thank Professor Alistair Standish, Course Coordinator of the Master of Biotechnology program at the College of Medicine and Public Health, Flinders University, for his valuable guidance, consistent support in lining up the thesis submission process, and mentorship throughout the year.

My gratitude to the SAHMRI Microbiome Team, specifically Dr. Joselyn Choo and DR. Andrew Shoubridge, for excellent technical assistance at crucial points in the study. My thanks are also extended to Alison Richards and Levi Elms familiarizing me with sophisticated laboratory protocols, which facilitated assay development and validation by qPCR.

To my lab mates in the HMRB Microbiome research group, I appreciate the camaraderie that created a positive and friendly atmosphere. Your friendship served to make each day in the laboratory a better and motivating experience. A special thank you to my lab mates and friends, whose support and shared frustration made the most challenging days endurable. Lastly, I owe a debt of gratitude to my friends and family. To my parents, thank you for not just believing in me but also supporting my education from day one. To my partner, I thank you for unconditional love, patience, and support you were my rock through those trying times.

This thesis is a culmination of the collective encouragement, mentorship, and support I have received from a group of amazing individuals to whom I owe my greatest gratitude.

Chapter One: Introduction

1.1 Overview

Cystic fibrosis (CF) is a severe autosomal recessive disorder caused by mutations in the CFTR gene, leading to multiple organ dysfunction especially in the respiratory and gastrointestinal systems. The thickened mucosal secretions and impaired mucociliary clearance in people with cystic fibrosis (pwCF) create an ideal environment for chronic respiratory infections, enabling a wide range of pathogens to colonise the airways. *Mycobacterium abscessus* Complex (MABC) is an emerging multidrug-resistant pathogen, that cause respiratory infections in pwCF. MABC is a non-tuberculous mycobacterium (NTM), consisting of three subspecies, *M. abscessus subsp. abscessus* (Maa), *massiliense* (Mam), and *bolletii* (Mab) (Davidson et al., 2021). MABCs are intrinsically resistant to multiple categories of antimicrobials and have been implicated in accelerated lung function decline, increased morbidity, and poor therapeutic outcomes.

The conventional diagnostic tests for detecting MABC in the lungs rely on culture-based tests and molecular tests. These tests have various drawbacks. MABC culturing is time consuming and can result in false negatives because of contamination with oral flora, biofilm production, or low bacterial loads in the sample. Obtaining sputum or bronchoalveolar lavage (BAL) samples can be quite challenging in paediatric pwCF or in individuals with severe pulmonary disease (Forton, 2015). These challenges delay accurate diagnosis and timely detection of bacteria, which is crucial for managing progressive pulmonary infection in pwCF.

In response to these drawbacks, recent research has investigated the role of blood-based molecular diagnostics using circulating cell-free DNA (cfDNA) tiny pieces of microbial DNA shed into the blood during an active infection. The use of cfDNA testing presents a less invasive and potentially more sensitive diagnostic process, particularly when respiratory samples are hard to collect. Although cfDNA-based assays have shown effectiveness in detecting mycobacterial diseases, including *Mycobacterium tuberculosis* (Huang et al., 2022) and *Mycobacterium avium* complex (Li et al., 2024), the utilisation of cfDNA for detecting MABC has not yet been well established.

The purpose of this research is to determine the specificity, sensitivity, and efficacy of chosen qPCR primer pairs for identifying MABC cfDNA in the serum of pwCF. This study employed

a comprehensive in silico and in vitro experimental approach to evaluate and validate the primers to identify the most effective qPCR assay for future diagnostic application in pwCF.

1.2 Cystic Fibrosis

1.2.1 Genetic mutation in the CFTR gene – causes multi-organ disruption.

Cystic Fibrosis (CF) was first identified in 1938 as a life-restrictive disorder with an autosomal recessive mode of inheritance. CF is caused by the presence of variants in both copies of the Cystic Fibrosis Transmembrane Conductance Regulator (CFTR) gene, located on chromosome 7. Each mutated copy is inherited from one parent, over 2000 mutations have been identified, with the most common being the F508 del mutation (Vallières & Elborn, 2014). Mutations in the CFTR gene affect the CFTR protein at multiple stages and can cause dysfunction or absence of this protein. CFTR dysfunction leads to disruption of ion transport in epithelial cells across various organs, leading to multiple complications (Pagin, Sermet-Gaudelus, & Burgel, 2020).

Figure removed due to copyright restriction.

Figure 1.1 - Multi Organ disruptions caused by CFTR gene mutation in Cystic Fibrosis (Ramananda, Naren, & Arora, 2024)

Dysfunction of CFTR protein affects several systems as outlined in **Figure 1.1.** Firstly, CFTR dysfunction affects the pancreas from birth, leading to pancreatic insufficiency and diabetes in adulthood. Reduced CFTR activity also disrupts salt recovery in sweat glands and mucosal secretory cells. As a result, mucosal organs (the gastrointestinal system, respiratory system, and reproductive organs) are heavily impacted by CF. In the gut, thickened mucosal secretions in the intestines lead to complications such as intestinal blockages and distal intestinal

obstruction syndrome (DIOS), caused by a partial or complete blockage of the intestines by thickened stool (Lavie et al., 2015). Respiratory complications emerge after birth, where CFTR malfunction leads to airway obstruction, chronic infections, and inflammation, ultimately resulting in severe lung diseases responsible for most CF-related deaths (Koehler et al., 2003).

1.2.2 Chronic respiratory disease in CF.

Chronic respiratory diseases are the leading cause of morbidity and mortality in pwCF, with most CF-related deaths being attributed to lung failure (Turcios, 2020). Mutation in the CFTR gene cause ion imbalances resulting in dehydrated mucus and impaired mucociliary clearance leading to mucus plugging, chronic bacterial colonisation and chronic inflammation inside the lung (Sin, Wu, & Man, 2005). The cycle of infection and inflammation in the CF lung leads to repeated pulmonary exacerbations, characterised by increased cough, sputum production, shortness of breath and reduced lung function. These exacerbations accelerate the decline in lung function, as measured by forced expiratory volume in one second (FEV1). Lung function decline is a major determinant of survival in CF (Harun et al., 2016). Patients with lower FEV1 values face an increased risk of hospitalisation and death due to respiratory failure. A mean annual decline in FEV1 of 1% to 2% is characteristic of pwCF. Individuals with FEV1 below 30% usually become candidates for lung transplantation (Wilkens et al., 2010). Recent data from the Australian, United States, and European CF registries indicate that more than 50% of the CF population now consists of adults, with the average age of pwCF gradually increasing. By contrast, paediatric deaths made up about 10% to 20% of total deaths in the year 2014, with 10.5% recorded in Australia,11.9% in the US, and 17.7% in Europe as reported in the literature (Zolin et al., 2018).

1.2.3 Pathogens that cause lung disease in CF.

In pwCF, lung diseases are primarily affected by chronic infections from a range of bacterial, fungal, and viral pathogens. Among the most common bacterial pathogens are *Pseudomonas aeruginosa*, *Staphylococcus aureus, Haemophilus influenzae and Burkholderia cepacia* complex. Chronic respiratory infections are highly prevalent in CF, with pathogens like *P. aeruginosa* playing a significant role in disease progression. Studies indicate that approximately 70%-80% of adult pwCF are chronically colonised by *P. aeruginosa*, a highly virulent pathogen that exacerbates lung function decline through persistent infection and inflammation (Malhotra, Hayes, & Wozniak, 2019). In addition to these common bacterial pathogens, pwCF are also susceptible to more complex infections caused by mycobacteria,

particularly non-Tuberculosis Mycobacterium (NTM). The most common NTM species causing pulmonary infections in pwCF are the slow-growing *Mycobacterium avium* complex (MAC), the rapid-growing *Mycobacterium abscessus* and *Mycobacterium kansasii* and in certain regions *Mycobacterium xenopi* and *Mycobacterium malmoense* (Johansen, Herrmann, & Kremer, 2020).

1.3 Characteristics and clinical implications of Nontuberculous Mycobacterium (NTM)

1.3.1 Nontuberculous mycobacterium (NTM)

NTM is a diverse group of mycobacterial species distinct from the well-known pathogens *Mycobacterium tuberculosis* (MTB) and *Mycobacterium leprae*. These species are ubiquitous in the environment, being isolated from soil, natural water sources, dust, and a variety of other habitats. Unlike *M. tuberculosis* and *M. leprae,* which are primarily transmitted between individuals, the NTM species are environmental organisms and are not usually transmitted between individuals.

NTM species can be divided into rapidly growing NTM and slow-growing NTM based on their distinct growth rates (Zhang et al., 2023). While the majority of NTM species do not cause any illness in healthy individuals, some strains are opportunistic pathogens and have a particular tendency to infect immunocompromised patients and those with chronic lung diseases. For instance, rapid-growing NTM cause disease in both healthy and immunocompromised patients. However, some species of NTM can cause disease even in otherwise healthy hosts. These species are associated with human diseases that typically manifest in the lungs, skin/soft tissues, lymphatic system or as disseminated infections. The two most common NTM species isolated were *Mycobacterium avium* complex and *Mycobacterium abscessus* (Zhou et al., 2022). This analysis points towards data in China, given its sheer size and diversity of population, and there is useful insight to be had in regional differences in prevalence and distribution of NTM. With extensive systems of surveillance and reporting in China, and increased awareness of infection by NTM, a strong epidemiological view can be applied to general global trends. **Figure 1.2** presents a breakdown of NTM detected in a study highlighting the distribution of NTM across different regions in China. The five most frequently isolated NTMs, accounting for 88.5% of all NTM cases, are *Mycobacterium abscessus* complex (MABC) (36.0%), *Mycobacterium avium-intracellulare* complex (MAC)

(34.1%), *M. kansasii* (9.8%), *M. paragordonae* (5.4%), and *M. lentiflavum* (3.2%) (Liu et al., 2021).

Figure removed due to copyright restriction.

Figure 1.2 - Distribution of non-tuberculous mycobacteria (NTM) species isolated from clinical samples in China, highlighting the relative proportions of rapidly growing mycobacteria (RGM) and slowly growing mycobacteria (SGM) (Liu et al., 2021).

1.3.2 *Mycobacterium abscessus* complex (MABC)

The *Mycobacterium abscessus* complex *(*MABC) is a group of rapidly growing, multidrug-resistant NTM bacteria that are responsible for a wide range of infections, including skin and soft tissue diseases, central nervous system infections, bacteraemia, and lung infections. Infections caused by MABC are particularly challenging to treat due to their resistance to antimicrobial drugs. MABC comprises a strictly aerobic, fast-growing mycobacterium, normally presenting in two well-defined morphologies of colonies on culture: one smooth, shiny type, most often recovered in wound infections; and a second rough, dry colony type, which is mainly found in pulmonary infections, especially in the airways (Park et al., 2015). The colonies, in general, are non-pigmented and do not stain well with Gram stain. Applied

Gram stain often discloses thinly staining, "ghost-like" beaded gram-positive bacilli, suggesting a possible mycobacterial infection. Definitive diagnosis is done by the Kinyoun stain, which demonstrates positivity for acid-fast bacilli, including MABS; even the detection of a single acid-fast bacillus is suspicious for Mycobacterium infection (Jeong et al., 2013). Unlike other bacteria, MABC possesses unique cell wall properties including a lipid-rich, impermeable barrier that limits drug penetration. However, MABC was first isolated from a knee abscess in 1952. Initially grouped with *M. chelonae*, *M. abscessus* was reclassified as a separate species in 1992. Despite ongoing debates about taxonomy, the MABC is now recognised to include three subspecies, *M. abscessus* subspecies *abscessus* (Maa), *M. abscessus* subspecies *massiliense* (Mam), *M. abscessus* subspecies *bolletii* (Mab) (Lee et al., 2015). Maa is the most commonly detected subspecies causing infection, accounting for 45%-65% of cases, followed by Mam 20%-55% and Mab 1%-18% with treatment outcomes varying depending on the causative organism (Koh et al., 2017).

1.3.3 *Mycobacterium abscesses* Complex in Cystic Fibrosis

Many species of NTM, including MABC, are considered opportunistic pathogens in pwCF and present serious clinical challenges. These infections can also vary from asymptomatic colonisation to severe and progressive lung disease, complicating an already complex clinical picture due to underlying CF-related bronchiectasis (Tippett et al., 2018). Severe, persistent infection is referred to as Non-Tuberculosis Mycobacterial Pulmonary Disease (NTMPD), which is defined as a chronic infection of the lungs caused by various NTM species, leading to progressive lung damage over time. NTMPD can manifest in different forms, primarily nodular bronchitis and cavitary disease, with each type presenting in unique challenges in diagnosis and treatment.

1.3.4 Prevalence of NTM infection in pwCF.

NTM infections have become an increasing concern among pwCF worldwide. Studies show that the prevalence of NTM among pwCF has been steadily rising, with regional and country-specific differences. However, NTM infections have been reported in most industrialised countries, with an incidence rate ranging from 1 to 1.8 cases per 100,000 inhabitants. MABC is responsible for approximately 5-20% of NTM infections **(Figure 1.3)** (Ramananda, Naren, & Arora, 2024).

Figure removed due to copyright restriction.

Figure 1.3 - Number of *M. abscessus* Clinical Isolates from Respiratory Sources Reported in the Literature (PubMed, 1992–2015). Map created with D&C-© Articque.

While the exact prevalence of Nontuberculous Mycobacterial Pulmonary Disease (NTMPD) in Australia is unknown due to the absence of national surveillance system, discrete studies indicate a growing trend, especially in individuals with cystic fibrosis (pwCF). Current evidence indicates both *Mycobacterium avium* complex (MAC) and MABC as the most commonly found species in the clinical context. However, National-level data on the infection rate of MABC are not available in detail.

In comparison, other nations' extensive data provide a picture of the increasing clinical utility of MABC. In the United States, the prevalence of NTMPD has increased significantly with MAC and MABC being the most common species isolated. Over 10 years (2010-2019) data from the CF Foundation patients registry revealed that the incidence of NTMPD rose by 3.5% annually with the northern region showing the highest incidence of MAC and the south leading in MABC infections (Marshall et al., 2023). A similar trend was observed in Germany, where the prevalence of NTM infections remained stable at 7.53% to 8.76% between 2016 and 2020, but MABC was the most prevalent species. Narrowing the focus to MABC infections is particularly concerning because they lead to more severe lung disease and prolonged infections compared to other NTM species (Steindor et al., 2023). In the United States, MABC accounted for 25.5% of all NTM cases among pwCF, while in Germany it was the most detected NTM species. In a CF clinic population study from 2002-2011, MABC was responsible for 46% of all NTM infections and was associated with prolonged infections and poor clinical outcomes

(Bar-On et al., 2015). These findings emphasise the global prevalence of MABC in pwCF emerging as one of the most common pathogens among NTM.

1.4 Clinical Challenges in MABC infection in pwCF

1.4.1 Treatment regimens and poor success rate.

Pulmonary infections with MABC are associated with more severe disease, longer treatment duration and higher rates of treatment failures compared to other NTMs. In pwCF, MABC infection can accelerate lung function decline and is often a contraindication for lung transplantation. Current therapeutic regimens are most often combined intravenous and oral antibiotics, with a trend towards aggressive multi-drug therapy that extends over a very prolonged period ranging from months to years. The usual regimen includes the use of macrolides, aminoglycosides, and beta-lactams, although their use is limited by MABC resistance (Jeon et al., 2009; Novosad et al., 2016). For example, it encodes an inducible macrolide resistance gene, *erm* (41), that significantly impairs one of the most prominent cornerstones of treatment, clarithromycin (Nash, Brown-Elliott, & Wallace, 2009). Moreover, *in vitro*, antibiotic susceptibility often correlates poorly with *in vivo* treatment outcomes, which renders it difficult to predict what drugs will work in specific patients. Despite prolonged and intensive therapy, the success rate of treatment remains low with cure rates ranging between 25% to 58% and many patients continue to experience chronic infections despite aggressive antibiotic therapy (Jonsson et al., 2007; Koh et al., 2017). Moreover, chronic infection is further complicated because many severe side effects arise due to the treatment itself, such as ototoxicity, hepatotoxicity, leukopenia, and gastrointestinal disturbances that most often result in discontinuation or adjustment of therapy (Novosad et al., 2016).

1.4.2 Monitoring MABC clearance during treatment.

Monitoring the clearance of MABC during treatment is crucial, as pulmonary infections with MABC in pwCF accelerate lung function decline, posing significant challenges to clinical management and often leading to antibiotic regimen failure. Therefore, careful monitoring of MABC clearance is essential for informed therapeutic adjustments and to evaluate patient eligibility for lung transplantation. Early and regular screening for MABC infection is important at various stages of the CF treatment. Typically, sputum culture results, combined with the patient's clinical presentation, are considered in decision-making. When such therapy fails or there is a partial response to treatment, the infection may persist with higher

consequences, one of which is macrolide resistance and poor long-term outcomes (Fairhurst et al., 2002). Regular monitoring of MABC clearance by the clinician allows them to assess the adequacy of the treatment regimen, evaluate the need for adjustment of therapy, and minimise potential complications resulting from possible disease progression or side effects caused by prolonged use of antibiotics.

Most serious cases of CF are generally considered for lung transplantation, but MABC infection creates a significant risk for complications after transplantation. Pre-transplant MABC infection has been associated with higher rates of surgical site infections and poorer outcomes, including mortality, in the post-transplant period (Garrison et al., 2009). Assessment of MABC clearance before transplantation thus becomes very important. Persistent infection with MABC may result in invasive disease, especially following the use of immunosuppressive medications post-transplantation. Many transplant centres consider active MABC infection to be a relative contraindication to lung transplantation for this very reason.

Studies have highlighted the importance of monitoring at the initiation of the treatment, including the initial identification of the causative organism and continuous tracking of disease progression alongside antibiotic therapy to optimise patient outcomes (Evans et al., 2025). By frequently assessing infection status, healthcare providers can make evidence-based decisions on discontinuing antibiotics once the bacterial infection has resolved, thus preventing unnecessarily extended treatment durations (Recchia et al., 2023). Additionally, pre-lung transplantation assessments can identify bacterial clearance, ensuring that patients are free from infection before surgery. However, the routine collection of sputum or Bronchoalveolar Lavage (BAL) samples poses challenges due to the invasive nature of these procedures and the difficulty some patients have in producing sputum. As a result, there is growing interest in exploring the potential of blood-based diagnostics to enhance the detection and monitoring of MABC infection (Steindor et al., 2015).

1.5 Detection of MABC in Lung Infection

1.5.1 Current detection methods.

The diagnosis of MABC still involves culture, which has traditionally been considered the gold standard, using selective media such as rapidly growing mycobacteria medium (RGM) and Middlebrook 7H11 agar (Preece et al., 2016). Such media are effective in isolating MABC and other mycobacterial species from clinical samples. Some of the molecular diagnostic

techniques include polymerase chain reaction (PCR) and whole-genome sequencing (WGS), which have identified MABC with a high degree of precision and speed. Here sputum or BAL samples are obtained from the respiratory tract and used to facilitate molecular diagnosis. For example, certain genetic markers such as the *erm* (41) gene or rRNA sequences can be targeted via PCR to distinguish the subspecies of MABC (Akwani et al., 2022). On the other hand, serological approaches, mainly the enzyme immunoassays targeting glycopeptidolipids (GPL), are promising diagnostic tools for MABC. These tests measure serum IgA antibodies against the GPL core antigens. The increased GPL-specific IgA may indicate infection activity, especially in pwCF, and help discriminate between NTM species (Sabin, Ferrieri, & Kline, 2017).

1.5.2 Limitations of existing diagnostic methods

There are several diagnostic methods for the detection of MABC; all of them have significant shortcomings, especially in the direct sampling method. There are four main limitations. The first one is that culture-based detection methods are considered the gold standard but are time-consuming, usually upward of 7-10 days for the detection of MABC (Rodriguez-Temporal et al., 2023). The next one is this depends on the availability of viable sputum or BAL samples that are difficult to obtain from patients, especially paediatric patients, or those with less sputum production. This challenge was highlighted in studies that reported a 20-day median time for culture positivity in MABC infections, with a median of 41 days for definitive identification (Park et al., 2022). The other limitation is contamination with other flora commonly present in the respiratory tract may interfere with MABC isolation, and the last one is the formation of biofilm complicates its detection in culture in case of chronic infection.

Serological methods include enzyme immunoassays targeting GPLs (Lopez-Roa, Esteban, & Munoz-Egea, 2022).They are less invasive but underdeveloped for routine application, and less reliable in patients with compromised immune systems **(Table 1.1)**. Additionally, serological tests can sometimes cross-react with other NTM, making it challenging to specifically diagnose MABC. Table 1.1 shows the comparison between direct sampling methods for the detection of MABC.

The issue of false positives and false negatives in identifying MABC is a significant challenge in clinical diagnostics, as shown by research on culture-based detection from direct sampling from the respiratory tract. For example, a retrospective observational study conducted at the Belgian National Reference Centre for mycobacteria reported an increasing number of false positive cultures submitted by peripheral laboratories over the study period (Soetaert et al.,

2019). Such findings underscore the need for improvement in reliable molecular diagnostics to accurately identify MABC, minimise false positives and negatives.

Table 2.1 - Comparison of direct sampling methods for MABC detection.

Sampling site	Sampling Method	Advantages	Disadvantages
Direct Sampling from Respiratory Tract	Sputum Collection	Non-invasive, easy to collect, commonly used for respiratory pathogens.	Quality depends on patient's ability to produce sputum, contamination with oral flora.
	Bronchoalveolar Lavage (BAL)	High diagnostic yield, useful for deep lung pathogens, minimises contamination from upper respiratory flora.	Invasive, requires sedation, potential complications such as bleeding, time-consuming.

1.6 Emerging molecular detection techniques

1.6.1 Cell Free DNA

Circulating cell free DNA (cfDNA) is short fragments of double-stranded DNA (~75–200 base pairs) that are not packaged in cells and are present in a number of body fluids such as blood and urine (Pietrzak et al., 2023). First identified in the blood plasma by (Mandel, 1948) in 1948, cfDNA is released to the circulation mainly through apoptotic and necrotic pathways, although NETosis and exosomal secretion have also been inferred to have roles. Its bioavailability is relatively short-lived (16 minutes to 2 hours), which points to its utility as a dynamic disease biomarker (Pietrzak et al., 2023). After entering the bloodstream, microbial DNA fragments are released actively or due to host immune responses, including bacterial killing or phagocytosis. cfDNA released in the bloodstream may originate from diverse anatomical reservoirs like the oral cavity, respiratory, gastrointestinal, genitourinary systems, or skin, all of which have been considered potential sites for bacterial translocation, particularly when integrity of the epithelium is compromised **(Figure 1.4)**. Chronic pulmonary inflammation and infection in CF cause extensive epithelial damage, increasing the likelihood of microbial translocation of the respiratory compartment to the bloodstream. The high vascularization of the lung tissue and the chronic immune response enhance the possibility that bacterial DNA, including that of MABC, enters the circulation. As a consequence, the bloodstream is a

minimally invasive matrix for the detection of such low abundance cfDNA (Pietrzak et al., 2023).

Urine provides alternative non-invasive sources, but blood is the most common source for cfDNA analysis. Urine is attractive due non-invasive collection. However, cfDNA in the urine is derived mainly from two sources; trans renal DNA (fragments filtered across the kidney from the circulation) and DNA released locally from cells of the urogenital tract. These DNA fragments are smaller, typically below 100 base pairs because they are subjected to renal filtration and nuclease digestion upon passage through the urine (Burnham et al., 2018).

Figure removed due to copyright restriction.

Figure 1.4 - Entry routes of cell free DNA into bloodstreams from various body niches. cfmDNA: cell-free microbial DNA. **(Pietrzak et al., 2023)**

Within blood-derived sampling, serum and plasma are two choices (Xue et al., 2009); however, plasma is the preferred matrix due to minimal contamination and superior analytical performance. Plasma kept in EDTA tubes circumvents the clotting process inherent in serum generation, which causes leukocyte lysis and contamination with high-molecular-weight genomic DNA. This makes plasma the more appropriate matrix for preserving the short, fragments required for high-fidelity detection (Saukkonen et al., 2008). Successfully, plasma

cfDNA has a uniform fragment length that is suitable for sensitive and reproducible analysis with qPCR or sequencing. Various comparative analyses have documented that cfDNA isolated from plasma produces greater fetal proportions, improved pathogen detection, and enhanced methylation-aided tissue mapping than cfDNA isolated from serum (Wong et al., 2016). Commercial cfDNA isolation kits like MagMAX™ and Quick-cfDNA™ are also designed for the optimal recovery of cfDNA from plasma, further affirming the role of plasma in diagnostics. This is critical for the detection of bacterial cfDNA, where the microbial DNA is at extremely low concentrations (often <10 copies/μL in plasma), where even trace contamination may dampen discoveries. Thus, EDTA plasma is advisable for the detection of microbial DNA in the diagnostics of sepsis, tuberculosis screening, cystic fibrosis related infection tracking, etc (Huttunen et al., 2011; Long et al., 2023). Its enhanced sensitivity, specificity, and lesser background noise render the plasma the best biological matrix for cfDNA-driven research.

1.6.2 Role of cell-free DNA in blood as a marker

The emerging molecular diagnosis and blood-based techniques form a very promising solution for these challenges. Ongoing studies focus specifically on the tracing of cfDNA, and immune markers present in the blood for quicker and more precise MABC detection **(Figure 1.5)**. cfDNA comprises small fragments of DNA that are released into the bloodstream, originating from various cells and microorganisms. The detection of microbial cfDNA in blood has emerged as a less invasive and efficient alternative method for diagnosing infections that traditionally require more invasive sampling methods (Hu et al., 2025). This approach offers notable benefits, especially for pwCF, where collecting respiratory samples can be challenging.

Figure removed due to copyright restriction.

Figure 1.5 - Schematic comparison of conventional and novel approaches for detecting *Mycobacterium abscessus*. The conventional method involves invasive respiratory sampling (e.g., bronchial aspiration) followed by culture and microscopic identification. The novel approach utilizes cell-free DNA (cfDNA) extracted from plasma, enabling less invasive, faster, and potentially more sensitive detection using quantitative PCR.

Numerous studies have highlighted the effectiveness of cfDNA in diagnosing mycobacterial infections. For instance, metagenomic next-generation sequencing (mNGS) of cfDNA in blood has been shown to accurately detect *Mycobacterium tuberculosis* (TB) in patients, including cases where traditional culture methods fail to provide definitive results (Park et al., 2022). Another study investigating plasma cfDNA as a non-invasive diagnostic tool for TB detection showed that in smear-positive adults it was 100% sensitive, while in smear-positive children the sensitivity was 75%. Specificity was 100% in both groups in whom TB was ruled out and in a large cohort of ambulatory controls (Pollock et al., 2021). This is an indication that *M. tuberculosis* cfDNA detection is highly specific and sensitive indicating that its presence in clinical testing should be considered definitive evidence of TB infection, warranting immediate treatment decision-making.

Similar results have been obtained with the detection of *Mycobacterium avium complex* (MAC) infections. A qPCR assay that includes a CRISPR guide RNA-based probe for detection of MAC from serum cfDNA was able to detect MAC with 97.6% sensitivity and 100% specificity.

The authors report this detection as a significant advance in less invasive diagnostic methods for mycobacterial infection (Li et al., 2024). This approach would also provide a lead to monitoring the efficacy of treatment, by tracking the levels of cfDNA during therapy, thus offering real-time insight into the patient's response toward the treatment. More research is needed regarding the application of cfDNA for detection in MABCs, but the existing literature provides a strong foundation for its clinical potential in less invasive diagnostics.

1.6.3 Quantitative PCR (qPCR) for MABC Detection in cell-free DNA

Currently, there are no qPCR-based methods to detect MABC from cfDNA. However, numerous MABC qPCR assays have been developed for detecting infections from respiratory samples, such as sputum. Their application for detecting MABS in cfDNA has not been established. One of the studies developed a quadruplex real-time quantitative PCR assay that could detect and differentiate MABC and MAC directly from sputum specimens without culturing (Dziedzinska et al., 2022b). This method was very sensitive and highly effective, thus enhancing the speed and accuracy of diagnosing pwCF with NTM; hence, it is suitable for routine clinical use. Another study found that Peptide nucleic acid (PNA) based qPCR assays performed even better than conventional ones, showing sensitivity and specificity of 96.7% and 100%, respectively, for the detection of MABC sputum samples. Because of these PNA probes, the detection could be done right from clinical samples without any necessity of extended incubation of culture; because qPCR was found to be an immense tool for diagnosis in fast-growing mycobacteria (Kim et al., 2015). However, as direct sampling methods have limitations in accuracy due to various factors discussed earlier, developing MABC detection in serum cfDNA is important for pwCF as it could provide a more accurate and less invasive diagnostic approach.

1.7 CRISPR-based Detection Methods

1.7.1 Potential for CRISPR in MABC detection

Management of mycobacterial lung infections is becoming increasingly prolific, particularly with the innovation of CRISPR/Cas systems such as CRISPR/Cas12a and CRISPR/Cas9. Among such recent developments is the ERA-CRISPR/Cas12a-based platform that couples CRISPR with enzymatic recombinase amplification (ERA) to allow ultra-rapid detection of MTB without the need for complex thermal cycling equipment (Gan et al., 2024). Notably, it demonstrated 100% specificity, showing no cross-reaction with other respiratory pathogens or

NTM (Sam et al., 2021). ERA-CRISPR/Cas12a showed perfect concordance in clinical trials with commercially available qPCR systems, and therefore, ERA-CRISPR/Cas12a is accurate, reliable, and can be used for diagnosing tuberculosis.

Besides tuberculosis, CRISPR technologies have been used in the study of NTMs (Xiao et al., 2020), including MAC a leading cause of pulmonary disease (PD) in those with predisposing conditions such as cystic fibrosis, where their lung health might already be compromised. An assay using CRISPR for the detection of MAC cfDNA in serum was developed. It provided a rapid diagnostic tool with great sensitivity for MAC PD. The sensitivity and specificity of the CRISPR MAC assay were 97.6% (Li et al., 2024). This assay also enabled the real-time monitoring of therapeutic efficacy. These findings show CRISPR technology is better when compared to most of the conventional diagnostic techniques in terms of speed and accuracy, hence offering important clinical benefits in the management of infections caused by MAC.

Applications of the CRISPR technologies are not limited to tuberculosis and MAC detection but have shown potential in the identification of a wide range of bacterial and viral respiratory pathogens. For instance, the adaptation of CRISPR systems has been made for detecting viral RNA, such as diagnostics relating to COVID-19 (Rahimi et al., 2021). Bacterial infection is very common and serious among patients suffering from cystic fibrosis; hence, recently CRISPR-based techniques have been increasingly used to cover rapid sensitive and specific detection for bacterial pathogen diagnosis to assist in timely treatment and monitoring. Importantly, this CRISPR assay could be adapted for detecting MABC infection in pwCF, providing an essential tool for managing and enhancing the detection of the vulnerable population.

This research focuses on addressing the pressing need for a more accurate, less invasive diagnostic tool for MABC infections in pwCF undergoing antibiotic therapy. below are the Hypothesis and research aims of this study,

1.8 Hypothesis and Research Aims

1.8.1 Hypothesis

Molecular diagnostic methods can be used to accurately detect *Mycobacterium abscessus* Complex (MABC) from cell-free supernatant from people with *M. abscessus* pulmonary infections.

1.8.2 Aims:

- **Aim 1:** Identify and select candidate primer sets from existing literature that target conserved regions of the MABC genome, ensuring suitability for qPCR-based detection. This step supports the hypothesis by ensuring specific amplification of MABC DNA.

- **Aim 2:** Evaluate the sensitivity, specificity, and reproducibility of the selected primers through qPCR using mock samples spiked with known quantities of MABC DNA (both unfragmented and fragmented). This will help determine the diagnostic performance and robustness of the assay.

- **Aim 3:** Design a CRISPR-Cas12a-based detection system targeting the validated qPCR amplicon to enhance post-amplification specificity and sensitivity.

- **Aim 4:** Validate the optimized qPCR assay using cfDNA extracted from mock plasma samples and, where possible, from clinical plasma samples of patients with confirmed MABC infection to assess its real-world diagnostic accuracy.

Chapter Two: Materials and Methods

2.1. Primer Selection

2.1.1 Literature Review and Primer Selection

As a first step, potential primer sets for qPCR-based detection of MABC were identified. A comprehensive literature review was conducted using scientific databases such as PubMed, Google Scholar, and Elsevier to achieve this. A list of candidate primers was compiled from previous research **(Table 2.1)**, particularly those targeting conserved gene regions in MABC, to ensure specificity and reliability.

Table 2.1 -Candidate Primers Targeting Conserved Gene Region in Mycobacterium abscessus Complex (MABC) for qPCR detection.

Primer Number	**Reference**	**Forward Primer (5' - 3')** **Reverse Primer (5' - 3')**	**Target site**
P1	(Nakanaga et al., 2014)	F- GGTAGCTCTTCCAGCCGAAT R -CAGCACGCA AAGGTACGAC	23S rRNA
P2	(Nakanaga et al., 2014)	F -GTCACCGCAGAAATCGAGTC R -GGGGTGGTTGACGTGTTC	23S rRNA
P3	(Macheras et al., 2009)	F-GAAGGAATCTCGTGGCTGAATAC R-AGTCGGCCTTGACGTTCTTGTAC	*sod*A
P4	(Macheras et al., 2009)	F-ACCAACGATGGTGTGTCCAT R -CTTGTCGAACCGCATACCCT	*hsp*65
P5	(Dziedzinska et al., 2022a)	F- GGAGTTCGTTGTGGATCTGG R-AAACCGTGAACGAAGGTGTC	*erm*41
P6	(Shallom et al., 2015)	F- GCGAAATTGCACTACGAGTAAAG R-CCTATCCTACACAAACCGAACC	23S rRNA
P7	(Shallom et al., 2013)	F -AGGCGGCCACCGACGTCGCGATGGA R -TGCGCCCGCCCAGCGCGTATCCG	*erm*41
P8	(Shallom et al., 2013)	F- GACTCCGGTGGCCGCGGCGA R-GCCGGAGCGCTGGGTGGGCT	*erm*41
P9	(Shallom et al., 2013) (Shallom et al., 2015)	F-GACCGGGGCCTTCTTCGTGAT R- GACTTCCCCGCACCGATTCC	*erm*41
P10	(Macheras et al., 2009) (Matsumoto et al., 2012)	F-GGCAAGGTCACCCCGAAGGG R- AGCGGCTGCTGGGTGATCATC	*rpo*B
P11	(Shallom et al., 2015)	F-GAGCATGGGCATATTCATGATGG R-TGAGCGAACACCGGATTCG	*erm*41
P12	(Shallom et al., 2015)	F- AGCGAAATTCCTTGTCGGGT R- CTGCTTCACAGTCTCCCACC	23S rRNA

P13	(Choi et al., 2011)	F- GAACACCTCAACCGCAGTG R- CATTAGCGCGATAGGCTCAC	VNTR loci
P14	(Choi et al., 2011)	F- CCTCGAGCCCAAGATCTGTC R- ATACCGGGATACGCCAAGAT	VNTR loci

2.1.2 In silico Analysis of Primer Sets

The in silico analysis was done to evaluate the suitability of the selected primers using computational analysis. To achieve this, Integrated DNA Technologies Oligo Analyzer (IDT) (Integrated DNA Technologies) and NCBI Primer-BLAST (Ye et al., 2012) were used to confirm specificity, ensuring that the selected primers did not align with non-target species. The Blast analysis was done, including three subspecies of MABC (Maa, Mam, and Mab), other Mycobacterium species such as *Mycobacterium avium*, *Mycobacterium intracellulare*, *Mycobacterium chelonae* and *Mycobacterium kansasii,* other common NTM pathogens including *Pseudomonas aeruginosa*, *Burkholderia cepacia, Haemophilus influenzae, Staphylococcus aureus,* and Human DNA.

In silico analysis was done by IDT and Oligo analyzer to assess various primer properties, including melting temperature (Tm), ensuring that each primer has a Tm within the optimal range of 55-65°C for qPCR. Secondary structures were analysed to check for potential hairpin formations and self-dimers, with primers having a $\Delta G \geq -3$ kcal/mol being avoided. Additionally, homo- and heterodimer formation has been examined, ensuring that the $\Delta G \geq -7$ kcal/mol to minimize non-specific amplification. Based on the in silico analysis, selection criteria, including minimal secondary structure and high specificity, were applied to filter out less suitable primers. The most promising primer sets had been recorded and ranked for further experimental validation.

2.1.3 Selection and Validation of Primer Sets

Use a Decision Tree **(Figure 2.1)** to guide the selection process based on Tm, specificity, dimer formation, and prior analysis. This structured approach identified six primer sets as the most suitable candidate for further wet laboratory analysis. These selected primer sets were then ordered from Thermo Fisher Scientific to proceed with experimental testing.

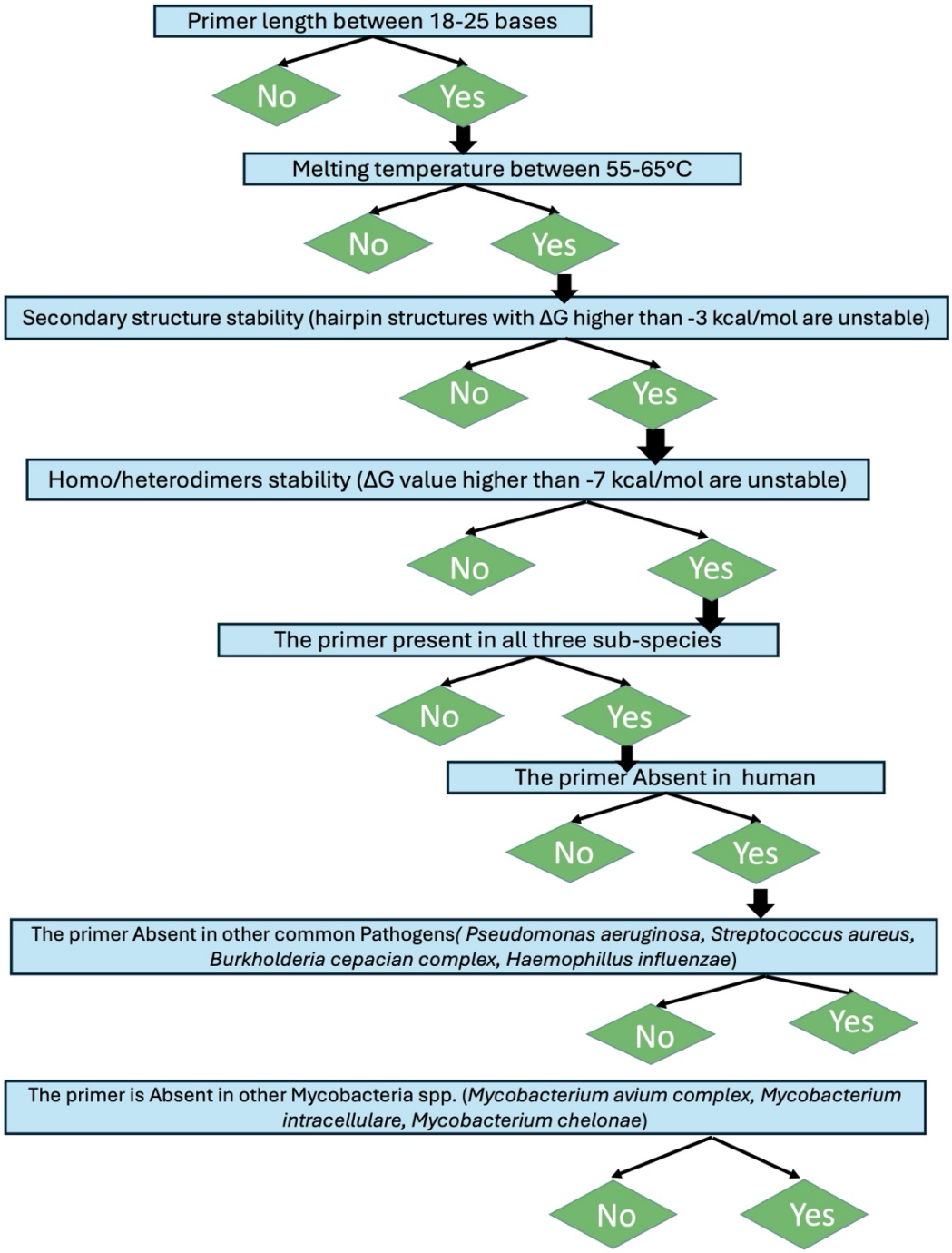

Figure 2.1- Decision tree for Primer selection based on melting temperature, Specificity, and dimer formation.

2.2 Specificity and Sensitivity Testing for the Selected Primer Sets

2.2.1 Specificity testing for selected Primers.

For specificity testing, target and non-target species bacterial DNA was acquired to test the performance of the selected primers in detecting MABC without cross-reactivity. The target bacterial strains were Maa, Mab, Mam, other non-tuberculous mycobacteria (NTM) were *M. avium, M. intracellulare, M. chelonae, M. kansasii,* and other common respiratory pathogens such as *Pseudomonas aeruginosa, Burkholderia cepacia, Haemophilus influenzae, Staphylococcus aureus*, and human genomic DNA. A 10-fold serial dilution was made for each of the bacterial strains for testing specificity with three dilution points being prepared to test primer performance at various concentrations of DNA. Each of the six selected primers was tested individually in qPCR runs to provide exact identification of MABC. The primer sets used, along with the corresponding PCR conditions, are provided in **Table 2.2.** The detailed PCR procedure followed for the analysis is here,

PCR conditions for detecting MABC using SYBR Green assay.

The qPCR assay detecting MABC was performed using the SYBR Green assay. Each reaction contained 0.7ul of each Primer (10mM), 1ul of DNA template, and 15.1ul of nuclease-free water, and 2X Platinum SYBR Green qPCR Master Mix (Applied Biosystems) and the appropriate volume of water was added to a 35µL total reaction volume. Quantitative RT-PCR was performed on three technical replicates, at 10 µL reaction volume per replicate, on a Quant Studio 6 Flex Real-Time PCR system (Applied Biosystems, Carlsbad, USA). Cycling conditions for SYBR Green qPCR assays for each primer set are presented in **Table 2.2.**

Table 2.2- Cycling Conditions for SYBR Green qPCR Assays of selected six Primer sets.

Primer Set	Forward Primer (5' - 3') Reverse Primer (5' - 3')	Initial Denaturation	Cycles	Denaturation	Annealing	Extension
Primer Set 1	GGTAGCTCTTCCAGCCGAAT CAGCACGCAAAGGTACGAC	95°C for 10 min	35	95°C for 1 min	55°C for 1 min	72°C for 1 min
Primer Set 2	GTCACCGCAGAAATCGAGTC GGGGTGGTTGACGTGTTC	95°C for 10 min	35	95°C for 1 min	55°C for 1 min	72°C for 1 min
Primer Set 3	GAAGGAATCTCGTGGCTGA ATAC AGTCGGCCTTGACGTTCTTG TAC	95°C for 2 min	35	94°C for 30 s	60°C for 30 s	72°C for 2 min
Primer Set 4	ACCAACGATGGTGTGTCCAT CTTGTCGAACCGCATACCCT	94°C for 1 min	45	94°C for 1 min	60°C for 1 min	72°C for 1 min
Primer Set 5	GGAGTTCGTTGTGGATCTGG AAACCGTGAACGAAGGTGT C	95°C for 7 min	47	95°C for 5 s	60°C for 40 s	60°C for 40 s
Primer Set 6	GCGAAATTGCACTACGAGTA AAG CCTATCCTACACAAACCGAA CC	95°C for 20 s	40	95°C for 10 s	60°C for 30 s	72°C for 30 s

2.2.2 Sensitivity Testing for the Selected Primers.

Two of the primer pairs had optimal amplicon size and high specificity for all three *Mycobacterium abscessus* subspecies. Based on this finding, the primer pairs were selected for sensitivity testing. To carry out the sensitivity testing, the concentration of bacterial DNA used in the reaction was quantified so that the number of copies of the DNA within each reaction was calculated with precision. This quantification was essential for determining the detection limits of the primers being selected. To measure the concentration of the DNA, the samples were quantified using Qubit fluorometric quantification to yield accurate and reliable concentrations of the DNA. A step-by-step procedure for the Qubit assay is detailed below,

Quantification of DNA using Qubit™ Fluorometer

The concentration of DNA was quantified using the Qubit™ 4 Fluorometer (Invitrogen, Thermo Fisher Scientific) and the Qubit™ dsDNA High Sensitivity Assay Kit (Cat. No. Q32851), following the manufacturer's instructions. The Qubit™ Fluorometer was calibrated before DNA samples were analysed, and a standard curve was prepared to ensure appropriate quantification. For the standard solutions, 10 µL of the Qubit™ standard solution was placed in the corresponding tubes, followed by the addition of 190 µL of Qubit™ working solution, which comprised 189 µL buffer and 1 µL fluorescent dye, to bring the final volume up to 200 µL per tube of standard. For the preparation of samples, 2 µL of each of the samples of DNA was loaded into individual tubes, to which 198 µL of working solution of Qubit™ containing 197 µL buffer and 1 µL of fluorescent dye were added to achieve a final reaction volume of 200 µL per tube. The tubes were mixed well following the addition of the reagents by vortexing at high speed for 3–5 seconds. The samples were allowed to stand at room temperature for 2 minutes to allow sufficient time for interaction between the reagent and the DNA. Following the incubation, the Qubit™ Fluorometer was used to read the standards and samples according to the manufacturer's protocol.

2.2.3 Calculation of copy numbers in the samples.

To determine the number of DNA copies, present in each qPCR reaction, the DNA concentration was converted into copy numbers using the formula.

$$\frac{Copies}{\mu L} = \frac{DNA\ concentration\left(\frac{ng}{ul}\right) x6.022x10^{23}}{(Genome\ size(bp)x1x10^{9}x650}$$

$6.022x10^{23}$ = Avagadro's Number (molecules/mol)

650 = Average molecular weight of one base pair (g/mol)

10^{9} = Conversion from ng to g

Genome size = in base pairs (bp)

The genome sizes of the organisms used in the study were obtained from published literature and are listed in **Table 2.3** below.

Table 2.3- Genome size of selected Mycobacterium species and their references

Organism	Genome size	Reference
Mycobacterium abscessus abscessus	5090491bp	(Cho et al., 2013)
Mycobacterium abscessus massiliense	4969787bp	(Cho et al., 2013)
Mycobacterium abscessus bolletii	5048007bp	(Cho et al., 2013)
Mycobacterium avium	4956929 bp	(Goethe et al., 2020)
Mycobacterium intracellulare	5402402 bp	(Kim et al., 2012)
Mycobacterium chelonae	5029817 bp	(Jaen-Luchoro et al., 2016)
Mycobacterium kansasii	6629039 bp	(Panda et al., 2017)

This approach allowed for precise standardization of input DNA in downstream sensitivity and specificity assays.

2.2.4 Creating the Standard Curve

Following this process, two primer sets were confirmed for sensitivity. Bacterial DNA copies per microliter were calculated by converting the concentration in ng/µL measured by Qubit fluorometric quantitation. A 10-fold serial dilution series was prepared for each sample, diluting the DNA concentration down to approximately one copy per microliter. qPCR assays were run with these dilutions to generate standard curves for each of the three subspecies of MABC. Comparison of the sensitivity of each of the primer pairs was achieved using qPCR with the generation of each primer's standard curve for determination of the linearity and quantification of the target at low concentrations of DNA. In addition to this, the qPCR assay efficiency was also determined for each of the bacterial strains.

2.2.5 Efficiency Calculation

To quantify qPCR performance for detection of various bacterial species, efficiencies were calculated for every assay based on the slope of standard curves produced by serial dilution of DNA templates. PCR efficiency served as an indicator of amplification performance, and an ideal 100% efficiency represented a target DNA doubling per cycle. Efficiency was calculated using the formula (Ruijter et al., 2021).

$$\text{Efficiency } (\%) = (10^{-1/\text{slope}} - 1) \times 100$$

2.3 Fragmented sample analysis

2.3.1 Fragmentation of DNA.

cfDNA, which under normal circumstances consists of fragmented DNA ranging between 75 and 220 base pairs, intact bacterial DNA was fragmented enzymatically to create a fragmented

DNA sample in all three subspecies of MABC. Controlled fragmentation was attained through the xGen IDT Library Preparation method that fostered uniformity and reproducibility of the fragment sizes. Fragmentation was performed using the xGen™ cfDNA & FFPE DNA Library Prep Kit (Integrated DNA Technologies, Cat. No. 10009861). The protocol for this fragmentation is outlined stepwise in below. Following fragmentation, the DNA was cleaned up to remove any remaining unwanted enzymes and reaction by-products to attain purity of the fragmented DNA. The cleaned fragmented DNA was aliquoted and stored at -20°C for further analysis.

DNA Fragmentation and Purification Procedure

In the preparation of the DNA samples, 1µL of each of the three MABC (Maa, Mab, Mam) were mixed with 19µL of EDTA TE buffer. This process was repeated twice to have two sets of each of the subspecies, resulting in a total of six prepared samples. The thermal cycler was set with the Enzymatic Prep program, and the lid temperature was set at 70°C. The enzymatic fragmentation reaction at 32°C lasted 22 minutes, followed by inactivation at 65°C for 30 minutes. The samples were then stored at 4°C to be further processed. Fragmentation times might be varied across lots of reagents, so optimization was performed by referring to the Certificate of Analysis (CoA) before proceeding.

Following the fragmentation, the Enzymatic Prep Master Mix was prepared by adding 3.0µL of Buffer K1, 1.5µL of Reagent K2, and 6.0µL of Enzyme K3 for a final reaction volume of 10.5µL per sample. The master mix was mixed well using a pipette, centrifuged briefly, and placed on ice until use. For full fragmentation, 10.5µL of the Enzymatic Prep Master Mix was added to each of the DNA samples in the 96-well plate for a total reaction volume of 30 µL per well. The samples were mixed 15 times using a pipette, centrifuged briefly, and then loaded directly into the cold thermal cycler to run the 32°C fragmentation step. The samples of DNA were then treated with magnetic bead clean-up following enzymatic fragmentation. The magnetic beads were first brought to room temperature, and 80% ethanol was freshly prepared. The beads were homogenized by vertexing, and 48µL magnetic beads (bead-to-sample ratio 0.8:1) per well were added. The samples were then mixed by pipetting 10 times, with pipette tips being replaced between samples. The plate was then left at room temperature for 5 minutes, before being placed on a magnetic stand for 2 minutes to allow separation of beads and supernatant. Once the supernatant had clarified, it was carefully discarded.

The beads were then twice washed with freshly prepared 80% ethanol to remove impurities efficiently. For each wash, 180µL of ethanol was added, the plate was left to incubate for 30

seconds, then the supernatant was removed carefully. Excess ethanol was removed with a P20 multichannel pipette. Following ethanol removal, the magnetic stand was removed, and 23µL of low EDTA TE was added to each well. The samples were pipette-mixed 10 times, tips being changed between samples. After 2 minutes of room temperature incubation, the plate was returned to the magnetic stand for 2 minutes to settle the supernatant. Finally, 20µL of purified DNA was transferred carefully to a tube and mixed. The fragmented DNA samples were then stored at -20°C to be processed further.

2.3.2 Assessment of fragmented DNA size distribution

To confirm whether the fragmented DNA was within the 100 bp to 220 bp range, the Bioanalyzer procedure was carried out following the Agilent 2100 Bioanalyzer System with the High Sensitivity DNA Kit (Agilent Technologies). The protocol was followed by one of our lab members with sample from other projects. The distribution of the fragment size was then confirmed using the Bioanalyzer by conducting electropherogram graphs, showing the successful fragmentation of Maa DNA. This was a quality check to see whether the DNA fragments were of the appropriate size for downstream applications.

Agilent High Sensitive DNA Kit Procedure

Preparing the Gel-Dye Mix

The High Sensitivity DNA gel matrix and dye concentrate were equilibrated to room temperature for 30 minutes before use. The dye concentrate was centrifuged briefly and then vortexed for 10 seconds to make it homogeneous. Then, 15µL of dye concentrate was transferred to a vial of high-sensitivity DNA gel matrix and mixed thoroughly for 10 seconds. The mixture of gel and dye was then loaded into a spin filter and centrifuged for 10 minutes at 2240 g and stored in darkness at 4°C until used.

Loading the Bioanalyzer chip

The High Sensitivity DNA chip was removed from a sealed pouch and placed on a priming station for chips. 9.0µL of gel-dye mixture was placed in the respective well on the chip. The priming station plunger was pressed for 60 seconds and then released. After a waiting time of a further 5 seconds, the plunger was slowly withdrawn to 1mL. Another 9.0µL of gel-dye mixture was placed in individual wells on the chip.

Loading the Marker, Ladder, and samples

After that, 5µL of High Sensitivity DNA marker was pipetted into each of the ladder and sample wells. 1µL of High Sensitivity DNA ladder was added to the ladder well and 1µL of each of the DNA samples was pipetted into separate sample wells. If there were any unused

wells, they were filled with 1µL of marker to test for chip functionality. The chip was then placed horizontally into the IKA vortex mixer and was vortexed for 60 seconds with a speed of 2400 rpm to evenly distribute the sample.

Running the Bioanalyzer Assay and Clean-up

The Agilent 2100 Bioanalyzer was configured by correctly inserting the electrode cartridge and placing the chip selector in position (1). The prepared chip was correctly inserted into the Bioanalyzer receptacle and closed with a light touch to prevent electrode breakage. The Expert Software 2100 was opened, and the right High Sensitivity DNA assay was selected. The file prefix and storage place were set, and sample details were entered into the sample table. The chip run was initiated by selecting the "Start" button and real-time acquisition was activated. After completion of the run, the used chip was removed and discarded in accordance with laboratory safety guidelines.

2.3.3 Quantification and standard curve generation for fragmented DNA

The concentration of fragmented DNA was measured using Qubit fluorometric quantitation, and copies per microliter were calculated for each sample. A 10-fold serial dilution series was created from fragmented DNA samples of all three subspecies of the MABC. The diluted samples were run using qPCR, and a standard curve was established to calculate the amplification efficiency and sensitivity of the assay for fragmented DNA. This approach offered accurate quantitation and confident detection of MABC DNA fragments at various concentrations.

2.3.4 Comparison of fragmented and unfragmented DNA Standard curves

Standard curves of fragmented and unfragmented DNA were compared to analyse variations in PCR efficiency, limit of detection (LOD), and slope for three subspecies of the MABC. PCR efficiency was calculated by the slope of the standard curves, and the limit of detection was determined by ascertaining the minimum concentration of DNA that could still be amplified consistently. Differences in amplification performance between fragmented and unfragmented DNA were compared to ascertain the impact of DNA fragmentation on qPCR sensitivity and quantitation accuracy.

2.3.5 Reproducibility testing

To evaluate the reproducibility of the qPCR assay using Primer set 6, intra- and inter-assay variability were assessed. For intra-assay testing, three technical replicates of each DNA concentration point were amplified within the same qPCR run. For the inter-assay testing, the

sample dilution series was amplified across three different runs on different days using identical reagents and a qPCR machine. Ct values were recorded for each replicate and the mean, standard deviation, and Coefficient of variation (CV%) were calculated to assess the reproducibility.

2.4 Fragmented MABC spiked mock plasma sample analysis.

2.4.1 Cell-free DNA extraction

To determine assay performance in controlled circumstances, mock plasma specimens were created through spiking fragmented bacterial DNA into healthy donor plasma. A healthy volunteer's whole blood was taken in EDTA-containing tubes and centrifuged at 2,000 × g for 10 minutes at 4°C to obtain plasma. Supernatant from the plasma was aliquoted into clean tubes and again centrifuged at 16,000 × g for 10 minutes at 4°C to eliminate residual cellular debris. Although the original study title referred to the use of serum, EDTA-treated whole blood was selected for plasma extraction in alignment with established best practices for cfDNA isolation. EDTA tubes are preferred due to their ability to minimise genomic DNA contamination and preserve short cfDNA fragments, which are critical for downstream molecular analysis. This approach is also consistent with prior *Pseudomonas aeruginosa* cfDNA studies (Long et al., 2023), further supporting its applicability.

The genomic DNA of *Mycobacterium abscessus abscessus* (Maa), *M. abscessus massiliense* (Mam), and *M. abscessus bolletii* (Mab) was fragmented **(Method 2.3)** and quantified using Qubit separately **(Method 2.2).** Separate aliquots of processed healthy plasma were each spiked individually with known quantities of each DNA fragment sample to prepare mock samples for each of the bacterial subspecies. The concentrations of the spiked DNA and the sampling strategy used for preparing mock plasma samples are detailed in **Table 2.4** and visually represented in **Figure 2.2**.

cfDNA was isolated from spiked plasma using the MagMAX™ Cell-Free DNA Isolation Kit (Thermo Fisher Scientific, Cat. No. A29319) according to the manufacturer's manual protocol described below.

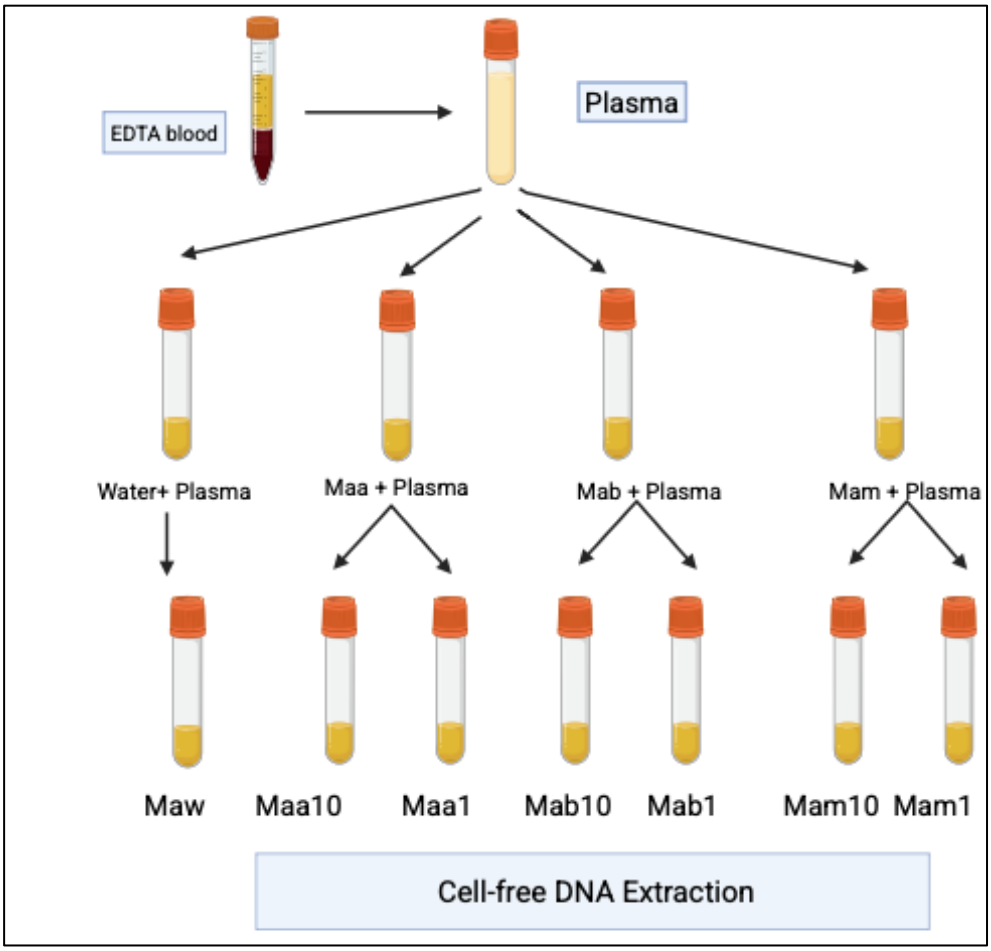

Figure 2.2 - Schematic workflow illustrating the preparation of mock plasma samples for cell-free DNA (cfDNA) analysis. Whole blood from a healthy donor was collected in EDTA tubes and centrifuged to isolate plasma. The plasma was aliquoted and spiked with fragmented genomic DNA from three *Mycobacterium abscessus* complex subspecies, *M. abscessus* subsp. *abscessus* (Maa), *M. abscessus* subsp. *bolletii* (Mab), and *M. abscessus* subsp. *massiliense* (Mam) at varying concentrations. Water-spiked plasma served as the negative control (Maw). Samples (e.g., Maa10, Maa1, Mab10, Mab1, Mam10, Mam1) were subsequently subjected to cfDNA extraction using the Mag MAX™ Cell-Free DNA Isolation Kit to evaluate assay performance under controlled conditions.

Table 2.4 - Concentrations of fragmented genomic DNA spiked into mock plasma samples for cfDNA analysis.

Sample name	Concentration of the spiked DNA
Water	0
Maa10	5.87ng/ul
Mab10	5.18ng/ul
Mam10	5.45 ng/ul
Maa1	0.587 ng/ul
Mab1	0.518ng/ul
Mam1	0.545 ng/ul

Mag MAX Cell-Free DNA Extraction Kit Procedure

Binding solution and bead mix preparation

1 mL of serum was mixed with 1.25 mL of Mag MAX Cell-Free DNA Lysis/Binding Solution and 15 µL of MagMAX Magnetic Beads to prepare 1x binding solution/bead mix. This mixture was added to the sample of serum and mixed well by inversion or swirling. In an effort to bind DNA as maximally as possible to magnetic beads, the mixture was subjected to rigorous vortexing for 10 minutes in a vortex adapter or microplate shaker at setting 7 or greater.

Bead separation and initial washing.

The tubes were left for about 5 minutes on a Dyna Mag 96 side™ magnet until the solution cleared and magnetic beads were pelleted. The supernatant was removed gently using the pipette and tubes were left for another minute on the magnet to eliminate the remaining liquid. Beads were resuspended in 1 mL of Mag MAX™ Cell-Free DNA Wash Solution and moved into non-stick 1.5 mL microcentrifuge tubes. Original bind tubes were saved for washing.

The tubes were returned to the magnet for 20 seconds following transferring and were used to rinse the original lysis/binding tube using supernatant. Leftover beads were combined in the new tube. Tubes were again held in position for 2 minutes using the magnet prior to removal of the supernatant. Beads were washed using 1 mL of 80% ethanol, and 30 seconds of vortexing was followed by 2 minutes of magnet separation. Ethanol was removed, and beads were air-dried for 3–5 minutes.

Elution and rebinding

Beads were resuspended in 400 µL of 0.1× TAE buffer and mixed by vortex for 5 minutes. Tubes were left to incubate on the magnet until the solution cleared. The supernatant eluate containing eluted cfDNA was pipetted into new microcentrifuge tubes. To increase yield, 5–10 µL of Mag MAX™ Magnetic Beads and 500 µL Lysis/Binding Solution were added to eluate. Mixture was shaken for 5 minutes for rebinding of cfDNA onto beads.

The tubes were then magnetically separated for 5 minutes, and the supernatant was removed. Beads were washed using 1 mL of Wash Solution and were separated on the magnet. Two successive ethanol washes using 1 mL of 80% ethanol each were done after removing the supernatant. Tubes were gently tapped 5 times against the bench to release any residual liquid, and ethanol was removed using a 200 µL pipette. Beads were air-dried in the magnet for 3–5 minutes.

Final elution of purified cfDNA

15 µL of the Mag MAX™ Elution Solution was used to elute the final purified cfDNA for each sample, after which they were subjected to 5 minutes of vortexing. Subsequently, 2 minutes' incubation of the tubes in the magnet was followed by collecting and transferring the clear supernatant with the cfDNA to a new microcentrifuge tube. The DNA can be used immediately, or at 4°C for 24hour storage or –20°C for long-term storage.

2.4.2 PCR amplification of the extracted DNA

Following the extraction Maa10, Mab10, and Mam10 samples cell-free DNA (cfDNA) was isolated using the MAG MAX™ cell-free DNA isolation kit. The purified DNA samples were subjected to qPCR analysis using the Primer set 6. DNA extracted from each sample was serially diluted to generate a standard curve for each target. These dilutions were used to assess amplification performance and calculate the qPCR efficiency.

2.5 CRISPR gRNA Design for MABC cfDNA Detection

2.5.1 Primers and Target Sequence Selection

To initiate CRISPR detection of *Mycobacterium abscessus* cfDNA, a conserved genomic region was identified. 23S rRNA gene-targeted primers (Primer set 6) were selected based on earlier validations of qPCR assays. These primers were applied to amplify a targeted genomic fragment, and the obtained sequence was recovered by aligning against the *M. abscessus* reference genome using NCBI GenBank. The amplified gene target is shown in the **(Figure**

3.10) This sequence was chosen to be used in the downstream design of CRISPR guide RNA (gRNA).

2.5.2 Guided RNAs design using CRISPOR.

The identified target sequence was entered into the CRISPOR web tool (crispor.tefor.net) to find candidate gRNAs. CRISPOR website has a scoring system, scores these derived gRNAs based on a range of efficiency metrics, such as the Doench 2016 score, Moreno-Mateos score, and updated Doench Ruleset 3 model. Specificity scores, such as the MIT Specificity Score and Cutting Frequency Determination (CFD) Score, were also assessed. Besides efficiency and specificity, CRISPOR also identifies the restriction enzyme site data were checked to help guide subsequent cloning and validation steps. Candidate gRNAs scoring high efficiency, high specificity, and low predicted off-target activity were shortlisted **(Appendix 1)** to undergo further analysis.

2.5.3 Off-Target Analysis

After selecting the top-ranked gRNAs based on efficiency and specificity scores, gRNAs were analysed their potential off-target activity in the human genome. Off-target interactions of the candidate gRNAs were predicted against the human genome by using CRISPOR **(Appendix 2).** Potential predicted off-targets were assessed using a measure of up to four mismatches in sequences. Only gRNAs that showed zero significant off-target cleavage activities in the human genome were chosen to proceed to further validation. It was essential to do this to avoid non-specificity of the assay as well as to ensure clinical safety when using human plasma samples.

For further confirmation of the specificity and efficiency of the shortlisted guide RNAs, a separate analysis was conducted using CHOPCHOP, a different CRISPR design website **(Appendix 3).** The highest performing guide RNA candidate, AGATGCTCGTTACGCGCGGCAGG, was identified, having no predicted off-target binding sites in the human genome. The same target sequence was also searched using a nucleotide BLAST (blastn) against the *Homo sapiens* genome database through NCBI **(Appendix 4)**. The cross-verification activity confirmed that the guide RNA target selected was not significantly aligned to human DNA, ensuring specificity of assay.

2.5.4 Final guided RNA selection

Based on accumulated evidence from CRISPOR, CHOPCHOP, and NCBI BLAST analysis, a guide RNA sequence, AGATGCTCGTTACGCGCGGCAGG, was finalized to be applied in further development of CRISPR-Cas12a assays. The gRNA was highly efficient, highly

specific, and free from anticipated human off-target impacts, hence a prime candidate to be used to identify *M. abscessus* cfDNA in plasma in patients with cystic fibrosis.

Chapter Three: Results

This chapter describes the experimental results of the study on the molecular detection of *Mycobacterium abscessus* complex (MABC) by using quantitative PCR (qPCR) and CRISPR-Cas technologies. The results are structured sequentially according to the experimental workflow set in the methodology.

3.1 Primer selection and in silico analysis of primer sets

Primer selection and in silico validation were performed by assessing the thermodynamic stability, structural integrity, and species specificity of 14 different primer sets selected from the literature (**Table 2.1**).

Table 3.1 In silico evaluation of primer sets for MABC complex detection. "ΔG" values represent Gibbs free energy, where less negative values. Yes = meets criterion; No = fails criterion.

Primer Number	Primer length (18-25bp)	Melting Temp between 55-65°C in both primers	Temperature mismatch less than 2°C difference	Hair pin structures ΔG = ≥ -3 kcal mol^{-1}	Homo dimers ΔG = ≥ -7 kcal mol^{-1}	Hetero dimers ΔG = ≥ -7kcal mol^{-1}
P1	Yes	Yes	Yes	No	No	No
P2	Yes	Yes	Yes	No	No	No
P3	Yes	Yes	Yes	No	No	No
P4	Yes	Yes	Yes	No	No	No
P5	Yes	Yes	Yes	No	No	No
P6	Yes	Yes	Yes	No	No	No
P7	Yes	No	Yes	Yes	No	Yes
P8	Yes	No	Yes	No	No	Yes
P9	Yes	Yes	Yes	No	No	Yes
P10	Yes	Yes	Yes	No	No	Yes
P11	Yes	Yes	Yes	No	No	No
P12	Yes	Yes	No	No	No	No
P13	Yes	Yes	Yes	No	No	No
P14	Yes	Yes	Yes	No	No	No

The thermodynamic and structural assessments of the 14 primer pairs are presented in **Table 3.1**. All primers satisfied basic design requirement of suitable length (18–25 bp) however, except for primers 7 an 8, all the other primers melting temperatures within the optimal qPCR

temperature (55–65°C). Except for Primer 12, in which demonstrated a melting temperature (Tm) mismatch of over 2°C between the forward and reverse primers; all other primer pairs showed compatible Tm values. Furthermore, the majority of primer sets showed no significant potential for hairpin structures or homo-dimer formation (ΔG ≥ -3 kcal mol^{-1} and ≥ -7 kcal mol^{-1}, respectively), and minimal risk of hetero-dimer formation (ΔG ≥ -7 kcal mol^{-1}). The hetero-dimer structure was detected in Primers 7, 8, 9 and 10 due to ΔG values of less than –7 kcal/mol, indicating probable primer-primer interaction. Based on this assessment, Primers 1, 2, 3, 4, 5 6, 11, 13 and 14 were found to be structurally stable and eligible for further experimental validation.

Table 3.2 In silico analysis of selected Primer sets against target and non-target organisms using NCBI primer BLAST.

Primer set	MABC	Human	*Staphylococcus aureus*	*Pseudomonas aeruginosa*	*Mycobacterium avium complex*	*Burkholderia cepacia*	*Haemophilus influenzae*	*Mycobacterium intracellular*	*Mycobacterium chelonae*	*Escherichia coli*	*Mycobacterium kansasii*
P1	✓	✗	✗	✗	✗	✗	✗	✗	✓	✗	✓
P2	✓	✗	✗	✗	✓	✓	✗	✓	✓	✗	✓
P3	✓	✗	✗	✗	✓	✗	✗	✓	✓	✗	✗
P4	✓	✗	✗	✗	✓	✗	✗	✓	✓	✗	✓
P5	✓	✗	✗	✗	✓	✓	✗	✓	✓	✗	✗
P6	✓	✗	✗	✗	✓	✗	✗	✓	✓	✗	✓
P7	✓	✓	✗	✗	✗	✓	✗	✓	✓	✗	✗
P8	✓	✗	✗	✓	✓	✓	✗	✓	✓	✗	✓
P9	✓	✗	✗	✗	✓	✓	✗	✓	✗	✗	✓
P10	✓	✗	✗	✓	✓	✓	✗	✓	✓	✗	✓
P11	✓	✗	✗	✗	✓	✓	✗	✓	✓	✗	✗
P12	✓	✓	✗	✓	✓	✓	✓	✓	✓	✗	✓
P13	✓	✗	✗	✗	✓	✗	✗	✓	✓	✗	✓
P14	✓	✗	✗	✗	✗	✓	✗	✗	✓	✗	✓

Results of in silico specificity analysis performed using NCBI Primer-BLAST for all 14 primer sets (indicated by a checkmark "✓" for a match and an "✗" for no significant match) **(Table 3.2)**. All primer sets aligned to MABC, validating their application as able to detect the targeted organism. However, non-target organisms were found to have different degrees of cross-reactivity. Primer sets 7 and 12 exhibited amplifications with human DNA, indicating potential cross-reactivity and reduced specificity for MABC detection. Conversely, primer sets 2, 5, 7, 8, 9, 10, 11, 12 and 14 displayed sequence alignment with several non-target speciesas such as *Pseudomonas aeruginosa and Burkholderia cepacia* and *Haemophilus influenzae* suggesting risk for false positives. Additionally, none of the primer sets showed alignment or amplification with *Staphylococcus aureus* or *Escherichia coli*, indicating high specificity against these non-target bacterial species. These observations were used in choosing the best specific and achievable primers for further validation experiments.

Integrating primer thermodynamic assessment, structural assessment, and specificity, the six best primer-pairing possibilities were ranked using the decision tree criteria described in the **Figure 2.1.** The six primer sets listed in **Table 3.3** were subsequently subjected to laboratory-based validation to further assess their performance and specificity.

3.2 Primers selected for wet Laboratory analysis.

Table 3.3 Selected primer sets for qPCR detection of MABC based on the In silico analysis.

Primer set Number for the wet laboratory test	**Forward Primer (5' - 3')** **Reverse Primer (5' - 3')**	**Gene**	**Amplicon size**
1	F-GGTAGCTCTTCCAGCCGAAT R-CAGCACGCAAAGGTACGAC	23S rRNA	909bp
2	F-GTCACCGCAGAAATCGAGTC R-GGGGTGGTTGACGTGTTC	23S rRNA	182bp
3	F-GAAGGAATCTCGTGGCTGAATAC R-AGTCGGCCTTGACGTTCTTGTAC	*sod*A	540bp
4	F-ACCAACGATGGTGTGTCCAT R-CTTGTCGAACCGCATACCCT	*hsp*65	440bp
5	F-GGAGTTCGTTGTGGATCTGGR- AAACCGTGAACGAAGGTGTC	*erm*41	124bp
6	F-GCGAAATTGCACTACGAGTAAAG R-CCTATCCTACACAAACCGAACC	23S rRNA	111bp

The six primer sets target genes identified as conserved or diagnostic within the MABC species, such as 23S rRNA, *sod*A, *hsp*65, and *erm*41. The amplicon sizes ranges from 111 bp to 909 bp. Primer sets 2, 5, and 6 produce short amplicons and are well suited for the detection of cfDNA. These primers were subsequently tested in the laboratory for specificity and sensitivity using genomic DNA.

3.3 Specificity testing results of the selected primers

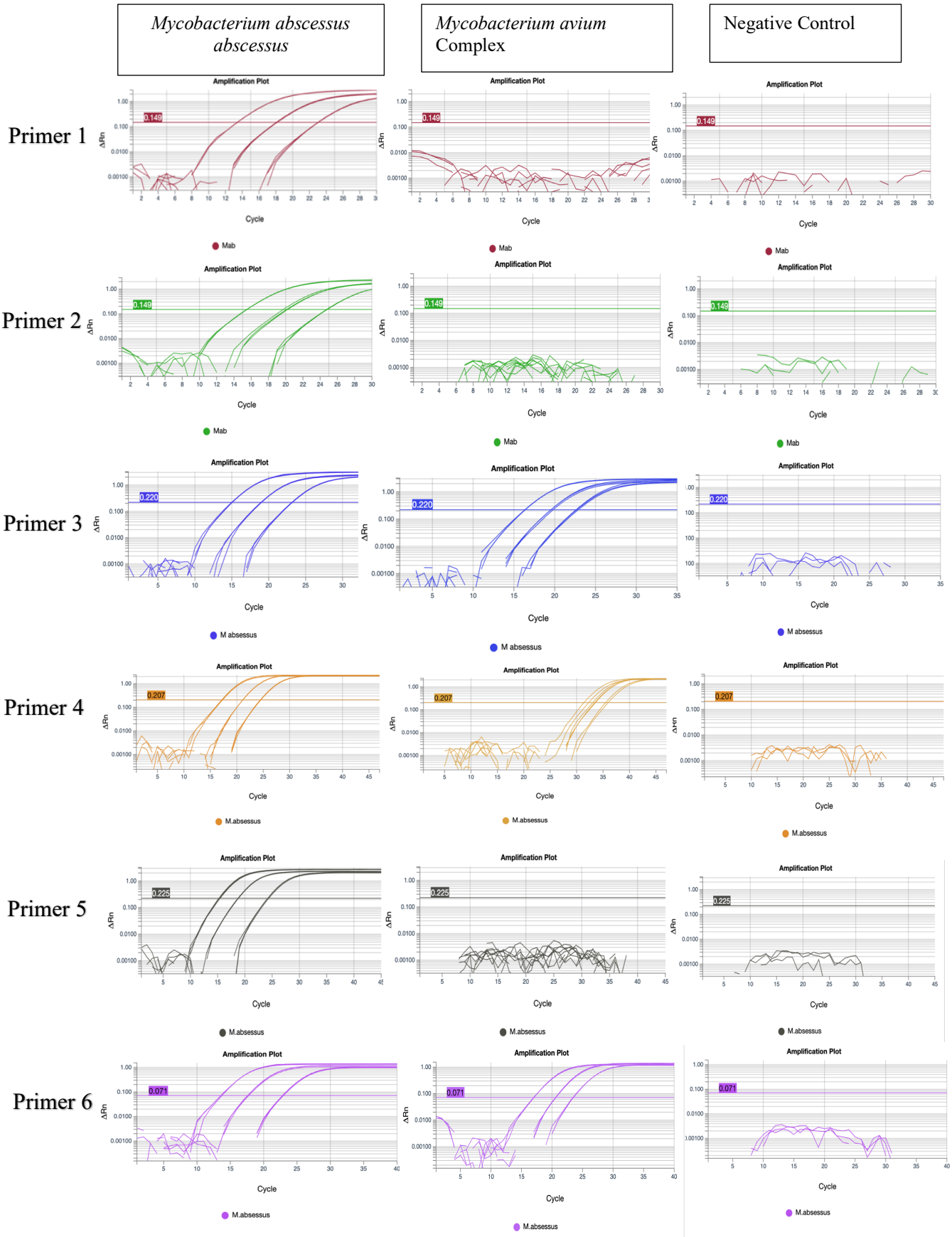

Figure 3.1 - Amplification curves of qPCR assays for selected Primer sets against Positive control, *Mycobacterium avium* Complex and Negative control. This figure presents qPCR amplification plots obtained for each selected primer set tested against *M. abscessus abscessus* positive control (left column), *M. avium* complex (middle column), and no template negative control (right column). Each raw corresponds to a different primer set. ΔRn (delta Rn) refers to the magnitude of normalized fluorescence signal after baseline correction. The X-axis shows qPCR cycle number, and the Y-axis indicates fluorescence intensity. Positive amplification is observed in the *M. abscessus abscessus* sample, while no amplification was detected in negative controls. *M. avium* complex was included among the tested organisms and demonstrated selective amplification, showing positive results with some primer sets while exhibiting no amplification with others,

	Mycobacterium abscessus abscessus	*Mycobacterium avium* Complex	Negative Control
Primer 1	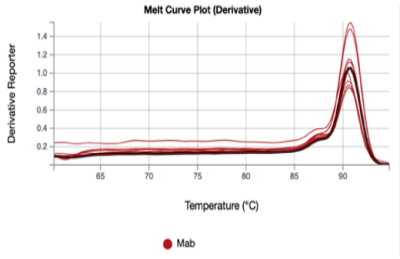	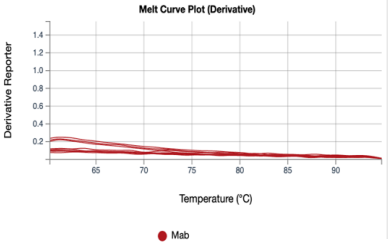	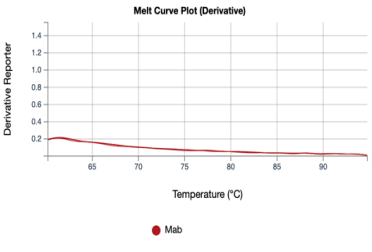
Primer 2	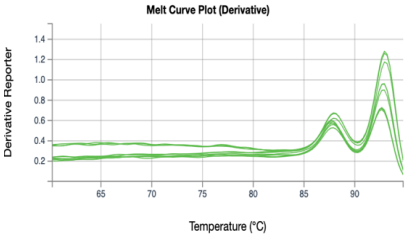	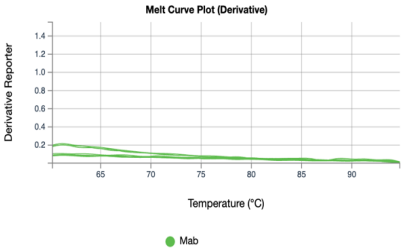	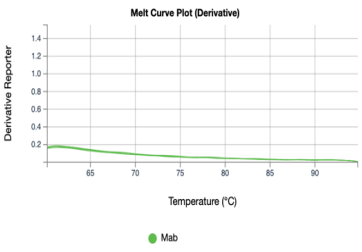
Primer 3	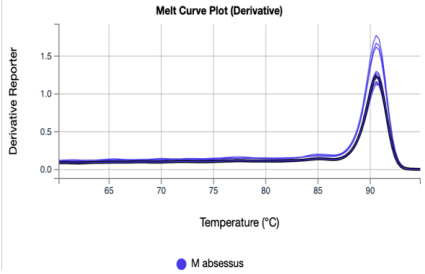	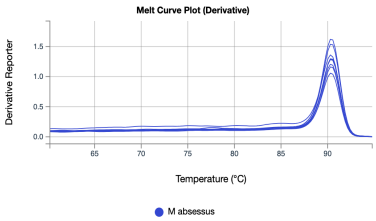	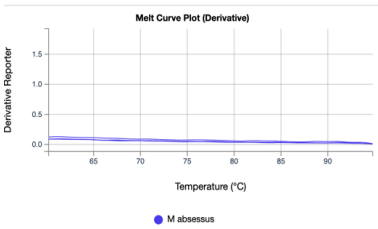
Primer 4	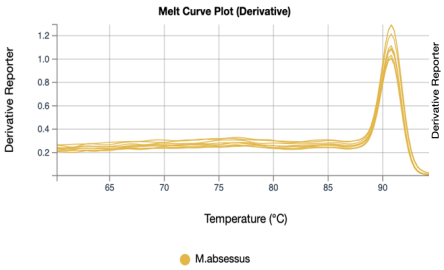	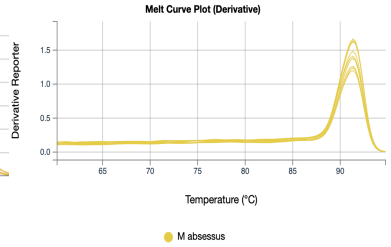	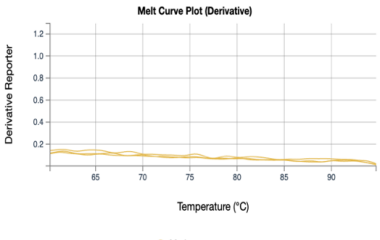
Primer 5	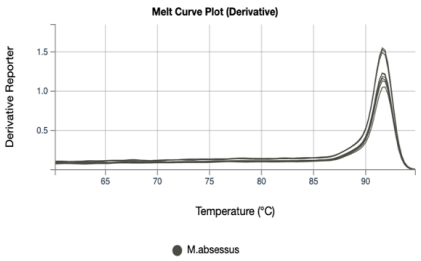	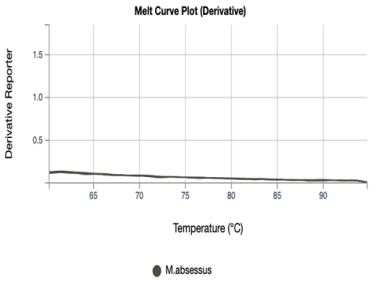	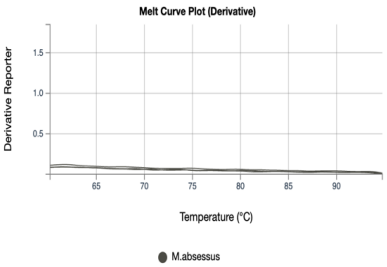
Primer 6	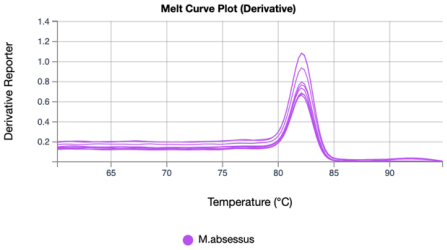	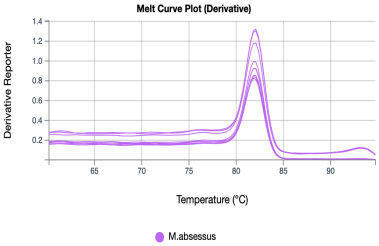	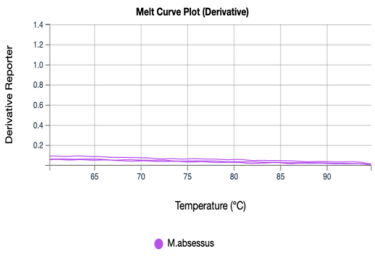

Figure 3.2 - Melt curves of qPCR assays for selected Primer sets against Positive control, *Mycobacterium avium* Complex and Negative control. The melt curve profiles displayed above demonstrate the six primer sets in *Mycobacterium abscessus abscessus*, *Mycobacterium avium* complex, and negative control samples. Each row represents results for one primer set, with corresponding melt curve profiles for the corresponding organisms.

Table 3.4 specificity results for the six selected Primer sets against target and non-target bacterial DNA.

Organism	Primer Set 1	Primer Set 2	Primer Set 3	Primer Set 4	Primer Set 5	Primer Set 6
M. abscessus abscessus	✓	✓	✓	✓	✓	✓
M. abscessus massiliense	✓	✓	✓	✓	✓	✓
M. abscessus bolletii	✓	✓	✓	✓	✓	✓
Staphylococcus aureus	✗	✗	✗	✗	✗	✗
Pseudomonas aeruginosa	✗	✗	✗	✗	✗	✗
Mycobacterium avium complex	✗	✗	✓	✓	✗	✓
Haemophilus influenzae	✗	✗	✗	✗	✗	✗
M. intracellulare	✗	✗	✓	✓	✗	✓
Mycobacterium chelonae	✗	✗	✓	✓	✓	✓
M. kansasii	✗	✗	✓	✓	✗	✓
E. coli	✗	✗	✗	✗	✗	✗

All six primer pairs successfully amplified DNA from the three targeted subspecies of MABC (*M. abscessus* subsp. *abscessus, massiliense,* and *bolletii*), demonstrating that the primers are capable of detecting MABC members. In contrast, no amplifications were found for non-related respiratory pathogens (*Staphylococcus aureus, Pseudomonas aeruginosa, Haemophilus influenzae,* and *E. coli*), which shows high specificity. Some cross-reactivity did occur with closely related non-tuberculous mycobacteria (NTMs), specifically with Primer Sets 3, 4, and 6, which did amplify *Mycobacterium avium* complex, *M. intracellulare, M. chelonae,* and *M. kansasii.* Primer Sets 1 and 2 showed the highest specificity, with no cross- reactivity observed against non-target organisms. Even though, Primer Sets 1 and 2 demonstrated the greatest

specificity, Primer Set 1 was not chosen because of its large amplicon size (909 bp), which is not ideal for detecting cell-free DNA fragments (usually 100–200 bp).

In addition, Primer Set 2 contained two melting peaks **(Figure 3.2, Primer 2)** within its melt curve profile, suggesting possible non-specific amplification. Thus, Primer Set 6, with an ideal amplicon size (111 bp), high specificity for all NTM species, and a clean melt curve profile, was chosen as the best candidate for further sensitivity trials. **Table 3.4** summarises the specificity testing results of six selected qPCR primer sets against DNA from both target and non-target organisms. A check mark (✓) indicates positive amplification, while a cross (✗) indicates failure to amplify.

Although the general reactivity of Primer Set 6 with several NTM species across several different species justifies the general utility for screening, its lack of strict specificity necessitates further refinements for target detection of MABC complex members. As a solution to this, the CRISPR-based improvement is to add a gRNA tailored to the 23S rRNA region that is amplified with Primer Set 6. The CRISPR-Cas12a system has the goal of enhancing the specificity of the assay to turn on fluorescence solely in the presence of MABC DNA to limit cross-reaction against non-MABC mycobacteria.

3.4 Sensitivity testing for the selected Primers.

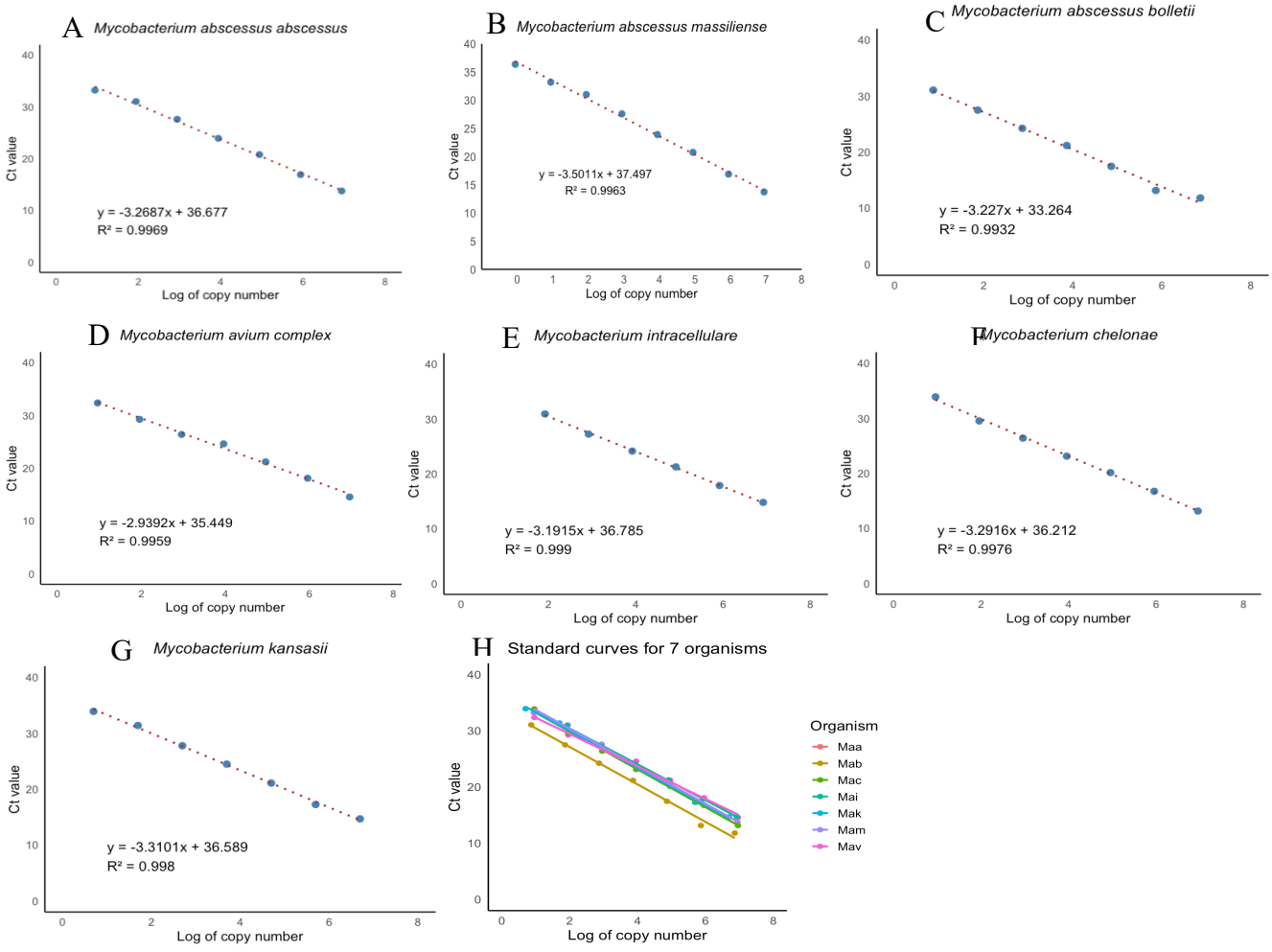

Figure 3.3 - Standard curve for seven organisms generated using primer set 6. Each graph shows the association of quantitation cycle (Ct value) with the log of copy number for target DNA, reflecting the amplification linearity and efficacy of the qPCR assay. Tested organisms include (A). *M. abscessus abscessus* (Maa), (B). *M. abscessus massiliense* (Mam), (C). *M. abscessus bolletii* (Mab), (D). *M. avium complex* (Mav), (E). *M. intracellulare* (Mai), (F). *M. chelonae* (Mac), (G). *M. kansasii* (Mak) and (H). all standard curves combine panel. All standard curves have high R^2 values (>0.99), reflecting good amplification linearity in the dilution series. The combined panel shows overlayed standard curves for visual relative comparison of performances among species.

The results in **Figure 3.3** present the sensitivity of the selected primer set 6 by constructing standard curves for DNA from seven different bacterial organisms, three subspecies of MABC including Maa, Mab, Mam and four non-target species Mac, Mai, Mav, Mak. Each standard curve showed a strong linear correlation between the Ct value and the log of the DNA copy number, with R^2 values above 0.99 for all organisms, indicating excellent qPCR linearity.

3.4.1 Standard curve linearity, efficiency, and limit of detection

The efficiency of the PCR indicates the amplification performance, with an ideal efficiency of 100% reflecting a doubling of the target DNA in each cycle. Efficiency was calculated using the formula (Ruijter et al., 2021) **(Methods 2.2.5)**.

Table 3.5 qPCR amplification efficiency and R^2 values for seven mycobacteria species using Primer set 6.

Organism	R^2 value	Efficiency %	Limit of Detection Copies/ul
Mycobacterium abscessus abscessus	0.9969	102.27	0.87
Mycobacterium abscessus massiliense	0.9963	93.04	0.94
Mycobacterium abscessus bolletii	0.9932	104.11	0.73
Mycobacterium avium	0.9959	118.89	0.95
Mycobacterium intracellulare	0.999	105.74	1.91
Mycobacterium chelonae	0.9976	101.28	0.90
Mycobacterium kansasii	0.998	100.94	4.95

Standard curves (from 10-fold serial dilutions of DNA template) of seven different species of Mycobacteria showed a linear pattern, with all standard curves having an R^2 of greater than 0.993 **(Table 3.5)** indicating strong linearity across all assays.

Notably, Maa, Mab and Mam exhibited robust amplification performance, confirming that Primer Set 6 is suitable for sensitive detection of all three MABC subspecies. Minimal variation

in amplification efficiency among species suggests that the assay is reliable for comparative analysis, even with low template concentrations.

The amplification efficiencies were between 90–110% for six out of seven species tested, indicating optimal qPCR performance. However, *Mycobacterium avium* exhibited an efficiency of 118.89%. However, despite this elevated efficiency, the assay maintained strong linearity (R^2 = 0.9959) for *M. avium*, suggesting that the observed deviation did not significantly compromise the standard curve's overall performance.

The Limit of Detection (LOD) was approximately 1 copy/µL for six of the tested species, while *M. kansasii* displayed a higher LOD (4.95 copies/µL), suggesting relatively reduced sensitivity for this organism. Collectively, the linearity, efficiency and LOD for Primer Set 6 indicate sufficient sensitivity across the three *M. abscessus* subspecies, as well as four other NTM species under the tested conditions.

3.5 Fragmentation of the DNA for sensitivity testing

3.5.1 Bioanalyzer results

A

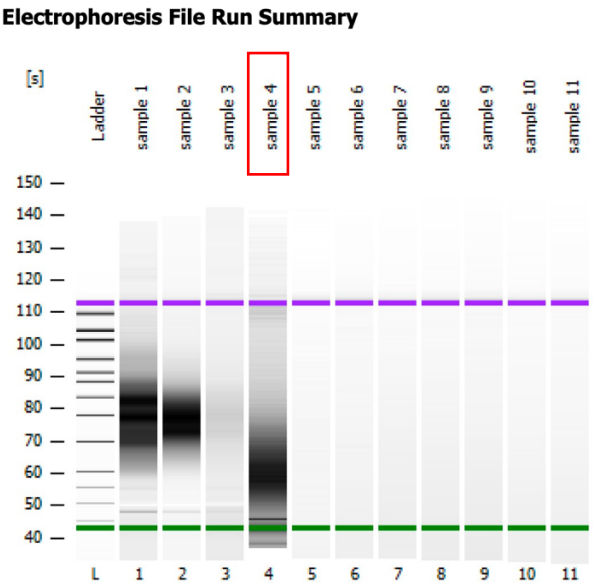

B

Assay Class: High Sensitivity DNA Assay
Data Path: C:\...gh Sensitivity DNA Assay_DE13806136_2024-11-20_13-30-19.xad

Created: 20/11/2024 1:30:19 PM
Modified: 20/11/2024 2:11:39 PM

Electropherogram Summary Continued ...

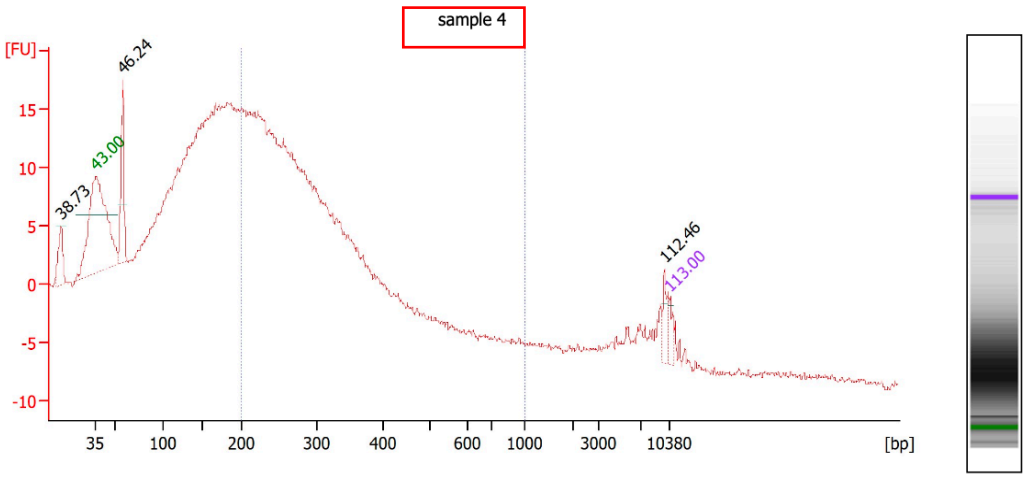

Overall Results for sample 4 : sample 4

Number of peaks found:	3	Corr. Area 1:	298.5
Noise:	0.3		

Peak table for sample 4 : sample 4

	Peak	Size [bp]	Conc. [pg/µl]	Molarity [pmol/l]	Observations
1		20.06308	0	0	
2	◀	35	125	5411.25	Lower Marker
3		57.48801	843.7576	22238.02	
4		9848.636	93.12982	14.32743	
5	▶	10380	75	10.94762	Upper Marker

Region table for sample 4 : sample 4

From [bp]	To [bp]	Corr. Area	% of Total	Average Size [bp]	Size distribution in CV [%]	Conc. [pg/µl]	Molarity [pmol/l]	Color
200	1000	298.4891	46.86838	280.9353	22.30248	12234.99	69457.19	

Figure 3.4 - Bioanalyzer results of fragmented DNA from *M. abscessus abscessus* (A) Electrophoresis gel image of the high-sensitive DNA ladder and sample 4, which represents fragmented DNA from *M. abscessus abscessus* following enzymatic fragmentation. Distinct bands indicate the successful fragmentation within the expected size range. (B) The electropherogram of sample 4 displays the fragment size distribution.

To simulate the physiological properties of circulating cfDNA found in human plasma, genomic DNA of high molecular weight was enzymatically cleaved. cfDNA is usually shed into the circulation via apoptotic or necrotic mechanisms and has short fragment sizes with a distribution skewed towards 75 to 220 base pairs (Snyder et al., 2016). The in vitro production of cfDNA like fragments was necessary to assess the sensitivity and specificity of the assay in a model that mimics clinical plasma specimens.

Fragmentation experiments were performed on purified genomic DNA extracted from three MABC subspecies (Maa, Mam, Mab) to simulate cfDNA characteristics observed in plasma. Agilent High Sensitivity DNA Bioanalyzer assay was utilized to analyse fragment size distribution and quality of enzymatically fragmented *Mycobacterium abscessus subsp. abscessus* (Maa) DNA. **Figure 3.4A** presents an electrophoresis Bioanalyzer run gel image, with sample 4 showing the fragmented Maa DNA. The clear smear between lower and higher markers is evident and reflects successful fragmentation of genomic DNA as required for cell-free DNA uses.

Figure 3.4B is an electropherogram for sample 4. The profile is that of a wide size distribution of DNA fragments, with a major peak at about 298 bp. It is interesting to note that the mean size distribution over that part of the range (200–1000 bp) sampled was 298.49 bp with a CV% of 32.30%. There is a smaller peak at 10380 bp continuing from this, most likely due to residual high molecular weight DNA that remains unbroken. Most fragments, however, were below 300 bp with a distinct concentration in the 75 –300 bp range.

This outcome indicates that the fragmentation protocol was successful in generating DNA fragments applicable to downstream qPCR assays, with a special emphasis on targeting short amplicons like Primer Set 6 (111 bp). The existence of cfDNA-sized fragments in the optimal detection range improves assay sensitivity and indicates high-quality input to molecular detection assays. Bioanalyzer assay confirmed that fragmented Maa DNA complies with size and quality standards for use in cfDNA detection-based applications, confirming that samples are suitable for further downstream tests.

3.5.2 Sensitivity testing after fragmentation of DNA.

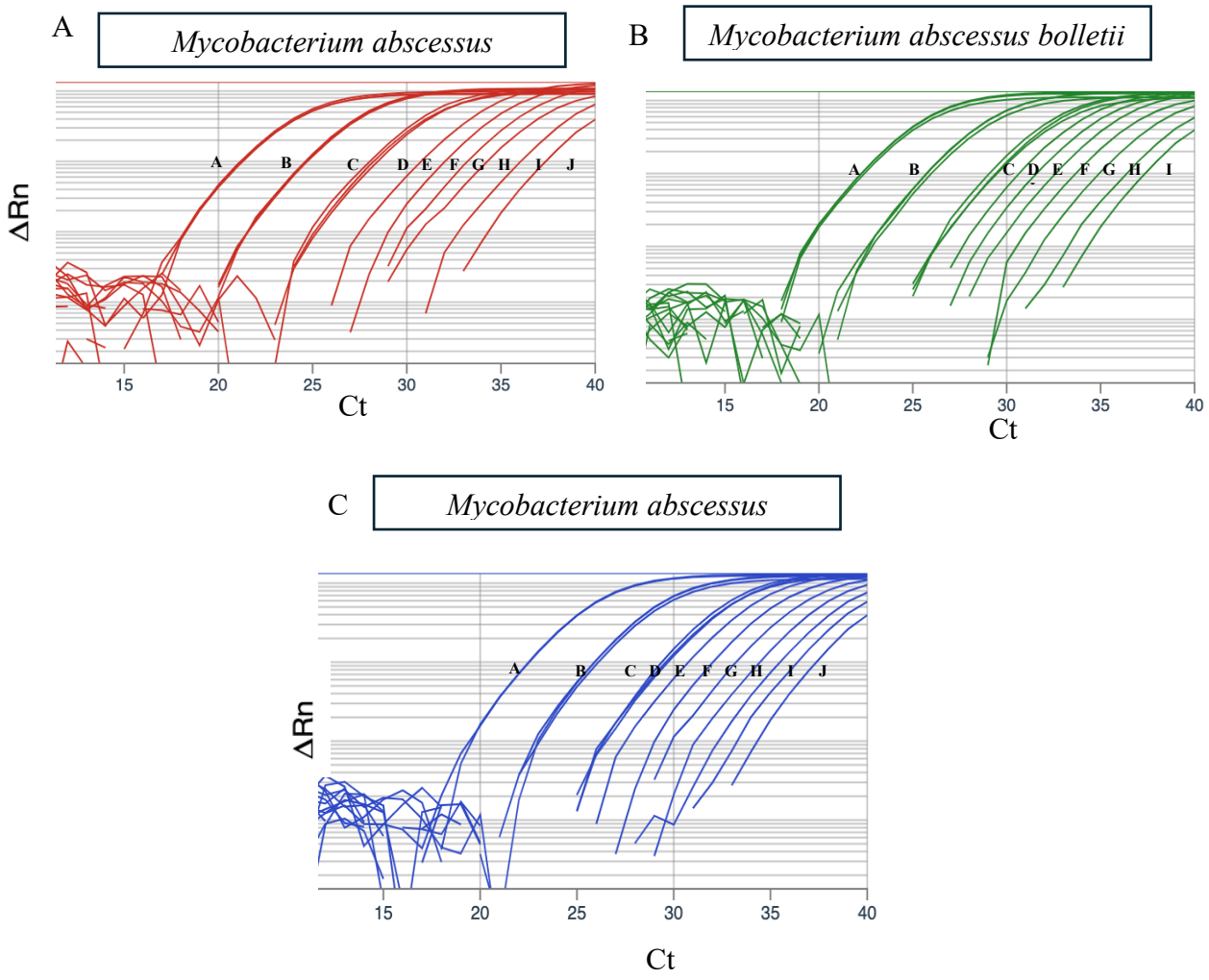

Figure 3.5 - Amplification Plots of Fragmented DNA from Mycobacterium abscessus Complex Subspecies Using Primer Set 6. Amplification curves generated by quantitative PCR (qPCR) following serial dilutions of fragmented DNA from (A) *Mycobacterium abscessus* subsp. *abscessus* (Maa), (B) *M. abscessus* subsp. *bolletii* (Mab), and (C) *M. abscessus* subsp. *massiliense* (Mam). Amplification plots of A-C represents 10-fold dilutions while C-J represents 2-fold dilutions. DNA fragmentation was confirmed by Bioanalyzer analysis, and DNA concentrations were determined by Qubit fluorometric quantitation. Standard curves were constructed from these data to evaluate assay efficiency, sensitivity, and the dynamic range for detecting fragmented MABC DNA.

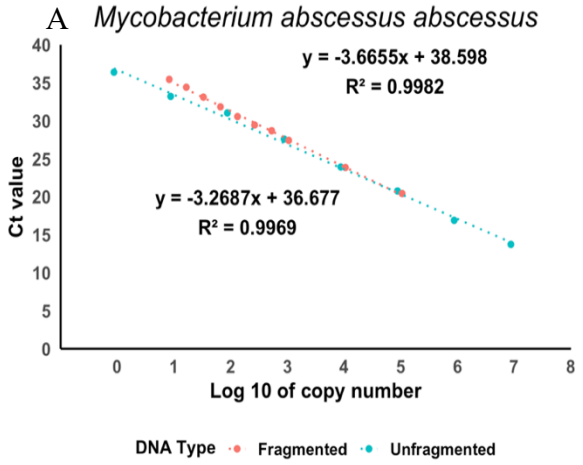

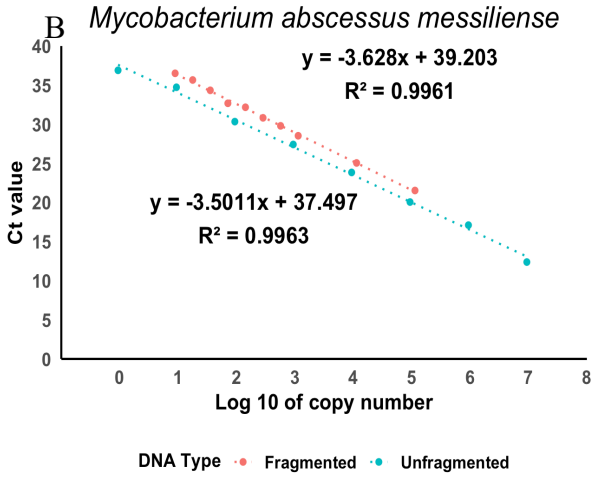

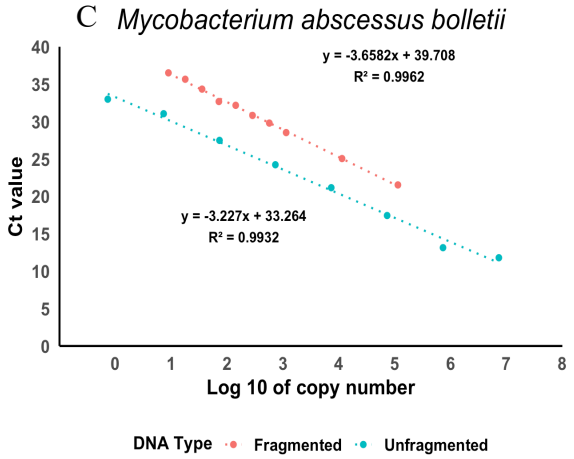

D Efficacy of the standard curve and the LOD after fragmentation

Organism	Efficiency %	LOD copies/ul
Maa	87.41	8.22
Mam	88.64	6.95
Mab	87.66	7.31

Figure 3.6 - Standard curves for qPCR detection of MABC before and after DNA fragmentation. Quantitative PCR standard curves were generated for unfragmented (blue) and enzymatically fragmented (red) genomic DNA from (A) *M. abscessus abscessus* (Maa), (B) *M. abscessus bolletti* (Mab), and (C) *M. abscessus messillense* (Mam). Each graph displays the linear regression of Ct values plotted against the logarithm of DNA copy number. Unfragmented DNA consistently demonstrated lower Ct values and steeper slopes, indicating higher amplification. Efficiency and sensitivity compared to fragmented DNA. Panel (D) summarises the qPCR efficiency and the Limit of Detection (LOD) for each subspecies following fragmentation.

Organism	Efficiency %	LOD copies/ul
Maa	87.41	8.22
Mam	88.64	6.95

The sensitivity of Primer Set 6 to MABC including (Maa, Mab, and Mam) fragmented DNA was determined using serially diluted enzymatically fragmented genomic DNA. **Figure 3.6** shows the qPCR amplification plot of the fragmented DNA, with panels A–C representing 10-fold dilutions and D–J representing 2-fold dilutions, reflecting uniform amplification within an extended dynamic range. Fragmentation of the DNA was confirmed using Bioanalyzer analysis **(Figure 3.4)** and the quantification of the DNA was determined using the Qubit fluorometry.

Figure 3.6 shows the comparison of standard curves of unfragmented and fragmented DNA. In all the subspecies shown, the fragmented DNA had greater Ct values and less steep slopes than unfragmented DNA, reflecting loss of amplification efficiency. This was to be anticipated because of the random strand breaks in the DNA, which may interfere with the binding of the primers and decrease the number of target regions available for amplification. Nonetheless, all standard curves were highly linear ($R^2 > 0.99$), which ensured the assay's stability.
As shown in **Figure 3.6D**, the calculated efficiencies of PCR after the fragmentation were 87.41% for Maa, 88.64% for Mam, and 87.66% for Mab. The corresponding LODs for each organism were 8.22, 6.95, and 7.31 copies/µL, respectively **(Figure 3.6 and Table 3.5).** Based on previous study, cfDNA concentrations in the blood of Mycobacterium *tuberculosis* affected patients ranging from 0.74 copies/µL (median) to a mean of 7.20 ± 29.15 copies/µL (Huang et al., 2022). This assay was designed with a target LOD of < 50 copies/µL of extraction to ensure diagnostic applicability. While fragmentation resulted in a slight decrease in PCR efficiency compared to unfragmented DNA, all three organisms maintained LODs within the clinically relevant detection threshold.

3.6 Reproducibility testing after fragmentation of DNA

3.6.1 Intra assay Reproducibility

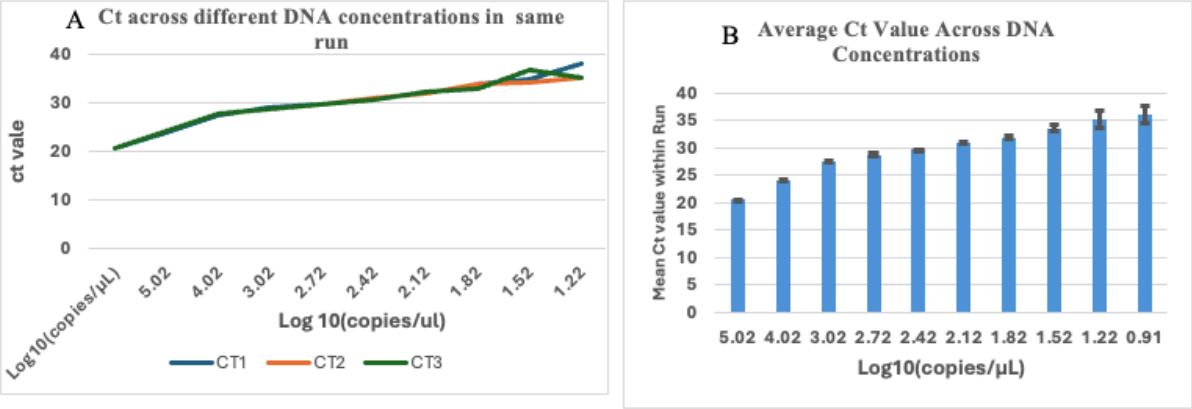

Figure 3.7 - Intra-assay reproducibility of the qPCR assay for Mycobacterium abscessus subsp. abscessus (Maa) detection using Primer Set 6. (a) CT values from three technical replicates (CT1, CT2, CT3) plotted against serially diluted DNA concentrations (log10 copies/µL), demonstrating consistent amplification across a dynamic range. (b) Mean Ct values with standard deviation error bars for each concentration, illustrating minimal intra-assay variability at mid-to-high DNA inputs and slightly increased variability at lower inputs. The coefficient of variation (CV) remained below 3% for both the highest and lowest concentrations, confirming excellent reproducibility in accordance with (Bustin et al., 2009) guidelines.

Figure 3.7A and **3.7B** collectively show the intra-assay reproducibility of the qPCR assay for Maa fragment detection with Primer Set 6. **Figure 3.7A** represents three technical replicates (CT1, CT2 and CT3) from a serial dilution series that have high concordance, especially for the middle to higher DNA input concentrations (5.02 to 1.82 $\log_{10}$ copies/µL). This close agreement reflects outstanding precision and consistent amplification proficiency within the same PCR run. There is only slight variation at the lowest point (1.22 $\log_{10}$ copies/µL), where CT1 deviates slightly (~38 cycles) from CT2 and CT3 (~35 cycles). This is an expected variance at the detection limit due to the amplification stochastic fluctuations at low abundance templates.

Figure 3.7B represents these observations by graphing the average CT for each concentration with error bars for standard deviation. The minimal error for higher concentrations indicates strong precision and repeatability, with error bars widening incrementally at decreasing concentrations consistent with the rising fluctuation at the assay's LOD. Additionally, the coefficient of variation (CV%) for both the highest and the lowest concentrations was less than

3%, which is acceptable based on the findings of (Bustin et al., 2009) findings for reproducibility. Combined, these findings demonstrate that the qPCR assay is highly reproducible within a run, especially for clinically relevant concentrations of DNA.

3.6.2 Inter assay Reproducibility.

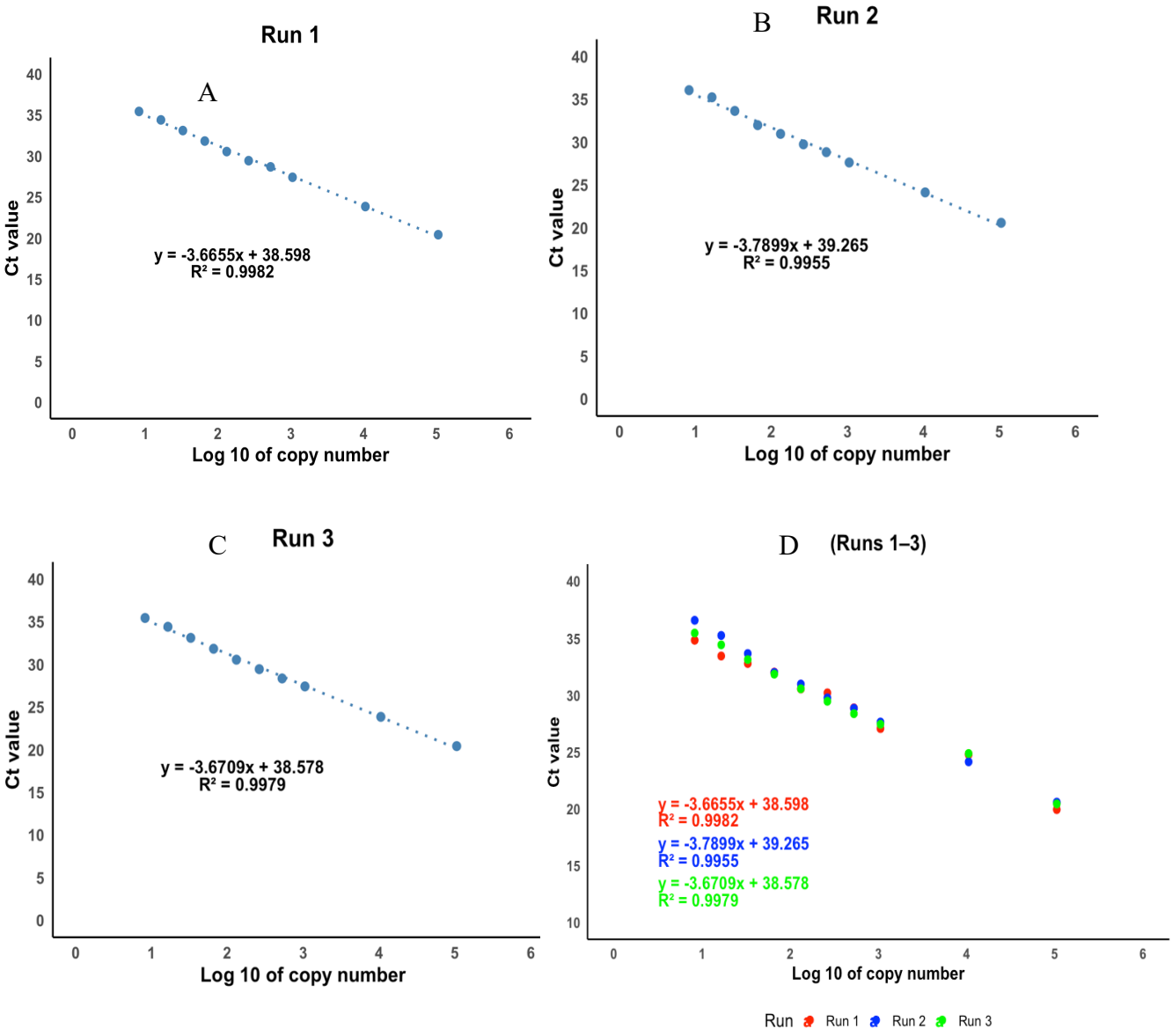

Figure 3.8 - Inter- run reproducibility of the qPCR assay targeting *Mycobacterium abscessus abscessus* using Primer set 6. Standard curves were generated from three independent qPCR runs using serial dilutions of enzymatically fragmented Maa DNA. Each panel (A-C) represents the Ct values plotted against the log10 of copy number for Run 1, Run 2, and Run 3, respectively. Panel D shows the overlay of all three runs, highlighting overall consistency while also revealing increased variability at lower DNA copy numbers. This variability, indicated by elevated standard deviations and coefficients of variation (CV), reflects the inherent stochastic fluctuations associated with low template concentrations in qPCR.

Table 3.6 Inter-run reproducibility statistics for standard curves generated from three independent qPCR assays.

Measurement parameters	Run 1	Run 2	Run 3	Mean	SD	CV (%)
Data for the slope of the Standard Curve	-3.6709	-3.7899	-3.5868	-3.6825	0.102	2.77
Data for the highest copy number	19.4912	20.5654	20.413	20.1565	0.5812	2.88
Data for the lowest copy number	35.0072	36.0574	34.4048	35.4371	0.8363	2.36

For evaluation of inter-run reproducibility, three separate qPCR assays were carried out using serial dilutions of Maa DNA that had been fragmented enzymatically. A standard curve was produced by each assay **(Figure 3.8A–C)** and the corresponding linear regression statistics were analysed. All three control curves exhibited very good linearity with $R^2 > 0.995$, indicating a robust relationship between Ct value and the logarithm of the DNA copy number. This extent of linearity is reflecting the quantitative accuracy and reproducibility of the assay over a large dynamic range.

The standard curves had a slope range of –3.5868 to –3.7899, showing high amplification performance. A further assessment of reproducibility was made using the coefficient of variation (CV%) for prominent parameters across the runs **(Table 3.6).** The CV for the standard curve slope was 2.77%, whereas the CV for the Ct at the highest and the lowest concentrations of DNA was 2.88% and 2.36%, respectively. These were all well within the acceptable range of <5% as suggested by the Minimum information for publication of Quantitative real time PCR Experiment (MIQE) guidelines (Bustin et al., 2009) that establish qPCR standards for precision and reliability criteria.

Together, these findings establish that the qPCR assay with Primer Set 6 is highly accurate and consistent across runs and within the runs. The reproducibility results demonstrate that the assay is suitable for clinical diagnostics, especially for the detection and tracking of MABC cfDNA within the context of plasma from pwCF.

3.7 Assessment of Primer 6 using serum spiked with fragmented MABC.

To evaluate the practical feasibility of the qPCR assay for the detection of MABC cfDNA in the pwCF mock plasma samples were made by spiking fragmented DNA from Maa, Mab, Mam into 1m aliquots of healthy donor plasma. Fragmented DNA was added at two concentration levels, high (~5.18–5.87 ng/µL) and low (~0.518–0.587 ng/µL), as outlined in **Table 2.4.** Following spiking, cfDNA was isolated with the MagMAX™ Cell-Free DNA Isolation Kit **(Methods 2.4)** Extracted cfDNA from each sample was amplified by Primer Set 6, and qPCR was conducted to construct standard curves and quantify assay performance.

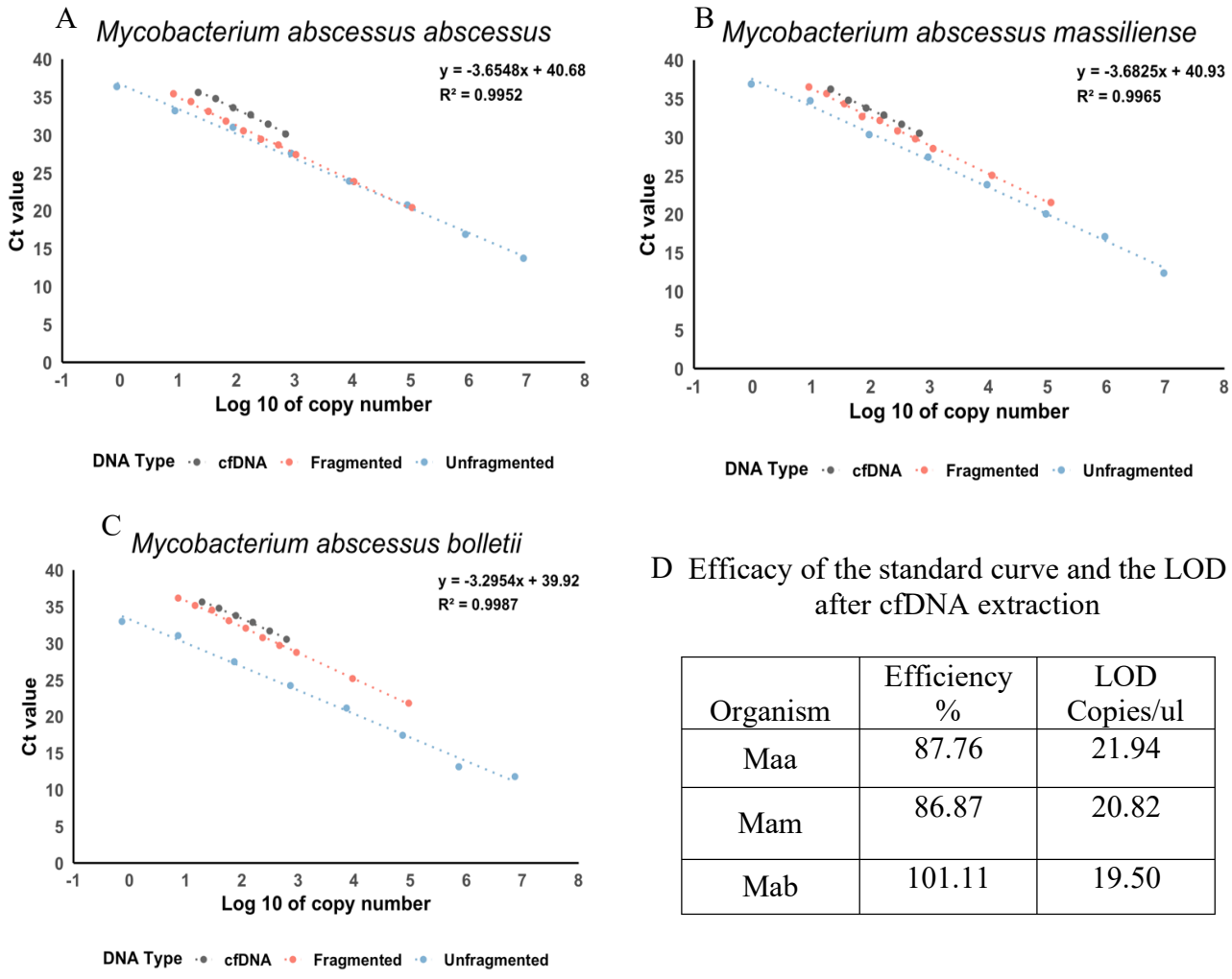

D Efficacy of the standard curve and the LOD after cfDNA extraction

Organism	Efficiency %	LOD Copies/ul
Maa	87.76	21.94
Mam	86.87	20.82
Mab	101.11	19.50

Figure 3.9 - Standard Curve performance of cfDNA from Mock Plasma samples Spiked with Fragmented DNA of MABC, comparison with Standard Curves from Fragmented DNA and Genomic (unfragmented) DNA. Quantitative PCR standard curves were generated for cell Free DNA (black) unfragmented (blue) and enzymatically fragmented (red) genomic DNA from (A) *M. abscessus abscessus* (Maa), (B) *M. abscessus bolletti* (Mab), and (C) *messillense M. abscessus* (Mam). Each graph displays the linear regression of Ct values plotted against the logarithm of DNA copy number. Unfragmented DNA consistently demonstrated lower Ct values and steeper slopes, indicating higher amplification. Efficiency and sensitivity compared to fragmented DNA. Panel (D) summarises the qPCR efficiency and the Limit of Detection (LOD) for each subspecies following cell free DNA extraction.

Figure 3.9 shows the comparison of the standard curves generated from cfDNA (black), enzymatically fragmented genomic DNA (red), and unfragmented genomic DNA (blue) across the three subspecies of MABC. The Ct values obtained from cfDNA samples were slightly higher than those from fragmented DNA, indicating a minor reduction in amplification efficiency likely due to matrix effects and potential loss during extraction. Notably, the cfDNA curves for Mam and Mab closely aligned with their corresponding fragmented DNA curves, demonstrating consistent performance. However, Maa exhibited greater deviation compared with the other two subspecies, with cfDNA samples showing comparatively higher Ct values, suggesting reduced template availability or more significant extraction-related loss in that subspecies. The LOD for cfDNA was higher in all organisms compared to fragmented DNA, reflecting the added challenge of recovering DNA from plasma at lower DNA concentrations. The efficiency of the cfDNA standard curves varied among the organisms, ranging from 87% to 101%, further indicating minor subspecies-specific differences in amplification dynamics in post-extraction.

Table 3.7 Comparison of observed and standard curve predicted Ct values for cfDNA extracted from mock plasma samples.

Sample Name	Copies/ul in reaction	Ct value
Maa1	70.095	32.95 (33.94)
Maa10	700.95	30.12
Mab1	62.42	33.07 (33.28)
Mab10	624.23	30.54
Mam1	66.656	33.63 (33.97)
Mam10	666.56	30.51
Maw	0	Undetermined

Table 3.7 summarise the measured Ct values (Black) obtained directly from qPCR analysis of mock plasma samples spiked with fragmented MABC DNA, alongside the predicted Ct values (red) calculated from corresponding standard curves. Samples including high (~5.18–5.87 ng/µL) and low (~0.518–0.587 ng/µL), concentrations for *M. abscessus subsp. abscessus* (Maa), *M. abscessus subsp. bolletii* (Mab), and *M. abscessus subsp. massiliense* (Mam). The water sample (Maw) served as a no template control and showed no amplification.

3.8 CRISPR gRNA design for MABC cfDNA detection

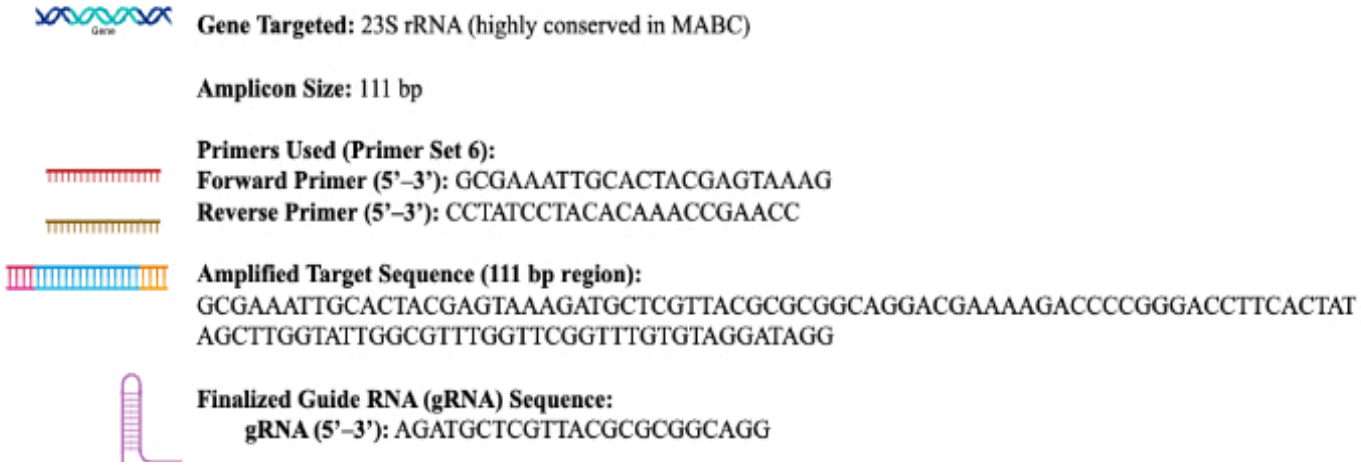

Figure 3.10 - CRISPR guided RNA (gRNA) design targeting the 23S rRNA gene of MABC.

While Primer Set 6 exhibited high amplification efficiency for all three subspecies of the *Mycobacterium abscessus* complex (Maa, Mam, and Mab), the primer also exhibited cross-reactivity with several non-target nontuberculous mycobacteria (NTM) species based on the specificity analysis. Such genomic reactivity, while useful for broad screening, restricts the diagnostic specificity for MABC detection. To overcome this limitation a CRISPR-Cas12a detection system was designed as an alternative strategy. The aim of this improvement is to enhance the specificity of the assay through the inclusion of a gRNA that is specifically designed to recognize a conserved motif within the 111bp 23S rRNA region that is complementary to Primer Set 6. The CRISPR-Cas12a enzyme is triggered only through specific hybridisation of the gRNA with the MABC target, facilitating collateral cleavage of a reporter molecule and generating fluorescence, thus reducing false positives due to the presence of the non-MABC NTMs.

The amplified sequence was aligned to the reference *M. abscessus* genome using NCBI GenBank, and the corresponding 111 bp target region was retrieved for downstream gRNA design. The selected region was then analysed using the tool, CRISPOR, to identify candidate CRISPR guide RNAs **(Appendix 1)**. Several high-scoring gRNAs were shortlisted based on CRISPOR scoring algorithms, and off-target analysis were conducted against the human genome to ensure nonspecific binding with human DNA. Only gRNAs with no significant off-target interactions (up to 4 mismatches) were considered. The top-performing gRNA sequence in **Figure 3.10**, AGATGCTCGTTACGCGCGGCAGG, was selected based on its high efficiency score and absence of predicted off-target effects.

Further validation of gRNA specificity was performed using the CHOPCHOP CRISPR design tool **(Appendix 2 and 3)** and NCBI BLAST (blastn) **(Appendix 4)** against the *Homo sapiens* genome. Both tools confirmed that the selected gRNA sequence did not significantly align with human DNA. In conclusion, the identified gRNA that is highly specific to the amplicon region of Primer 6, forming a suitable candidate for testing the CRISPR-Cas12a approach for MABC detection from cfDNA.

Chapter Four: Discussion

This study presents the development and evaluation of a qPCR assay optimized for detection of MABC in cfDNA from cystic fibrosis individuals (pwCF). Current culture-dependent approaches for MABC detection take 7–14 days and their sensitivity remains suboptimal, particularly for individuals unable to readily sputum. This research addresses this important diagnostic gap by providing a rapid molecular approach that can be applied to blood samplesThis study developed and evaluated a less invasive molecular diagnostic strategy for detecting MABC infections using cell-free DNA (cfDNA) from plasma. By combining quantitative PCR (qPCR) with preliminary design of a CRISPR-based enhancement, the research aimed to improve the sensitivity and specificity of detection of MABC in pwCF where sputum-based testing is often challenging. The diagnostic performance of 14 primer sets was assessed through in silico analysis, followed by wet-lab validation of six candidates using both intact, fragmented and Mock plasma cfDNA templates. Primer Set 6 emerged as the most promising candidate, though with acknowledged limitations in species specificity. The study further evaluated assay performance using clinical samples and proposed future improvements through CRISPR-Cas12a integration for enhanced diagnostic precision.

4.1 Primer screening and in silico analysis of primer sets

In silico analysis represents a crucial step prior to the laboratory validation. This initial filtering guarantees only the most suitable primer candidates those most likely to produce efficient and specific amplification in wet laboratory. Accordingly, this study integrated in silico analysis as a foundational step to select optimal primer sets for accurate and sensitive qPCR-based detection on MABC cfDNA in plasma samples from pwCF. Several primer sets from the literature did not satisfy the in silico analysis requirements. These included primers containing Tm mismatches, high values of ΔG and the tendency to form a heterodimer, showing lower amplification specificity and stability **(Table 3.1)**. In comparison, previous research underlined that the secondary structures with $\Delta G \geq -3$ kcal/mol tend to form more readily under standard PCR conditions with an influence on both sensitivity and specificity (Fredman et al., 2004; Thornton & Basu, 2011). More restrictive thresholds used in the current analysis provide a conservative approach towards high-fidelity amplification (Johnston et al., 2019). Furthermore, all primer sets demonstrated successful alignment to MABC targets in Primer Blast analysis (Ye et al., 2012), confirming their diagnostic relevance, though with varying degrees of cross

reactivity to non-target organisms. These observations align with previous work, which underscore the utility of in silico specificity analysis of primer sets in the early stages of primer validation (Wang, 2015; Ye et al., 2012). NCBI Primer-BLAST has proven efficient in the swift identification of candidate off-target alignments in complex metagenomic or clinical sample matrices BLAST (Ye et al., 2012). This observation is echoing the concerns expressed by (Blauwkamp et al., 2019) that even short regions of high-copy human genomic element homology compromise the reliability of the PCR test when analysing the cfDNA of bacteria in blood. The observations justify continued dependence Primer-BLAST as a front-line filter with regards to both target specificity and epidemiology robustness. The experimental validation of six primer sets targeting MABC confirmed their ability to amplify DNA from all three subspecies Maa, Mab and Mam demonstrating the assays' inclusivity across clinically relevant MABC strains. Notably, none of the primers successfully amplified DNA from unrelated respiratory pathogens other than NTM species **(Table 3.2)**. It is consistent with the existing evidence of the high genetic correlation between MABC and other NTMs of conserved genes such as *sod*A, *hsp*65, and 23S rRNA (Bensi, Panunto, & Ramos Mde, 2013; Singh et al., 2020). Collectively, the in silico analysis served as a critical gatekeeper in the development of a diagnostic qPCR assay for MABC detection.

4.2 Optimizing qPCR primer selecting and specificity analysis for MABC.

Designing a qPCR assay for detection of MABC using cfDNA requires particular attention to the amplicon size and target specificity. cfDNA is typically fragmented, as it is the result of apoptotic and necrotic cellular activity, and most of the released fragments circulate in the range of 75-200 base pairs (Pietrzak et al., 2023). Selecting primers that yield amplicons well within the typical cfDNA fragment range is essential for maximizing assay sensitivity and reliability, particularly in low-template scenarios such as early infection or post-treatment monitoring. Accordingly, primer evaluation in this study progressed beyond initial in silico screening to include targeted optimization for qPCR performance using cfDNA templates. (Ungerer et al., 2022). As shown by (Chen et al., 2024) long amplicons tend not to amplify reproducibly in cfDNA-abundant matrices, causing impaired sensitivity and unstable performance of the test. Primer set 2 had suitable amplification size however the melt curve revealed multiple peaks, indicating non-specific amplification **(Figure 2.2 Primer 2)**. This finding aligns with the work by (Guion et al., 2008), which demonstrated that secondary melt peaks are associated with non-specific amplification and can be considered a red flag for qPCR

validation. (Ruiz-Villalba et al., 2017) further highlighted that nonspesific melt signals, even those that are minor, can compromise the validity of a diagnostic test, especially if it is being used for high-sensitivity assays like pathogen detection from sputum or blood.

Primer set 6 was identified as the most suitable candidate due to its optimal amplicon size (111bp), high specificity to MABC and clean melt curve but exhibited cross reactivity with non-targeted NTM species **(Table 3.4).** This limitation is likely attributed to the high sequence conservation in the 23S rRNA gene, which has traditionally been targeted by broad-range mycobacterial assays owing to its diagnostic sensitivity. While this region's evolutionary conservation within multiple NTMs typically serves to reduce specificity, as aligned with the research by (Ruiz-Villalba et al., 2017). These investigations highlighted the recurring trade-off in qPCR assays between broad detection capability and species-level discrimination**,** especially when conserved 23S rRNA genes are used as targets. As per (Bensi, Panunto, & Ramos Mde, 2013) assays based on the targeting of conserved sequences successfully detected *Mycobacterium spp.* but often could not differentiate between closely related phylogenetic taxa, and thus resulted in false-positive interpretation.

Although Primer Set 6 showed optimal amplification efficiency and was successfully validated across all three MABC subspecies, a key limitation remains its inability to distinguish MABC from other closely related NTM species due to its target within the conserved 23S rRNA region. This non-specific amplification may compromise its diagnostic value in polymicrobial or NTM-endemic environments, where accurate species-level detection is critical. While this trade-off was mitigated by the short amplicon size (111 bp) suitable for cfDNA detection, future refinements such as the incorporation of downstream CRISPR-Cas12a detection—are essential to improve species discrimination. This limitation highlights the need to balance inclusivity with specificity in primer selection.

To overcome this specificity challenge, emerging innovations in CRISPR-Cas systems provide promising solutions **(Figure 3.10)**. By combining CRISPR-Cas12a-mediated detection and qPCR, specificity can be achieved after amplification. The Cas12a enzyme, guided by a sequence-specific gRNA, cleaves a fluorescently labelled reporter only if the amplified DNA exactly matches the target sequence (Chen et al., 2024; Huang et al., 2022). Through the collateral cleavage mechanism, an added verification step minimizes off-target amplification-derived false positives. The recent work has reported the success of the hybrid method in plasma detection of Mycobacterial DNA under demanding conditions like low abundance of DNA or high levels of background noise. For instance, (Huang et al., 2022) employed a CRISPR Cas12a based system to detect low abundance of *M. tuberculosis* cfDNA in plasma

demonstrating high sensitivity and specificity even in immunocompromised populations like HIV infected adults and children. Similarly, the recent study (Li et al., 2024) used CRISPR enhanced molecular assay to accurately identify *M. avium* Complex infections by targeting cfDNA, a challenging analyte due to its fragmented nature and low concentrations. The hybrid qPCR-CRISPR detection system is a new and promising approach to overcome cross-reactivity issues for microbial diagnosis (Chen et al., 2021). It supports an emerging trend in molecular testing toward integrating broad-spectrum amplification methods with highly specific post-amplification technologies. Future developments of the assay could be significantly enhanced by CRISPR-Cas12a integration to achieve the dual goals of high sensitivity and precise species discrimination. This section thus represents a pivotal step in refining a diagnostic tool tailored to the complex biological and clinical landscape of MABC infection detection in pwCF.

4.3 Analytical sensitivity assessment of Primer set 6.

Assessing the analytical sensitivity of a qPCR assay is essential for determining its performance across different biological contexts that mimic clinical conditions. Analytical sensitivity was evaluated through a three-phase approach using increasingly clinically relevant conditions. This included: (1) testing with intact genomic DNA **(Figure 3.3)**, (2) enzymatically fragmented DNA to simulate cfDNA-like properties **(Figure 3.6)**, and (3) cfDNA extracted from uninfected plasma samples spiked with fragmented MABC DNA **(Figure 3.7)**. This stepwise design enabled a comprehensive comparison of qPCR sensitivity across matrices of increasing biological complexity (Koskinen et al., 2009). Importantly, this approach not only captured the influence of DNA integrity on amplification efficiency but also evaluated the real-world impact of plasma-derived matrix effects and DNA recovery limitations (Shen et al., 2018). Although the original study title referenced the use of serum, EDTA-treated whole blood was selected for plasma preparation in accordance with best practices for cfDNA extraction. Existing literature supports the use of EDTA-treated blood for cfDNA extraction because as it inhibits nuclease activity and restricting cellular lysis to keep short cfDNA fragments intact for precise molecular diagnosis (Devonshire et al., 2014; Long et al., 2023).This progressive model enables a comprehensive evaluation of assay performance, capturing the influence of DNA integrity, matrix complexity, and potential interference from plasma-derived inhibitors.

4.3.1 Standard Curve linearity

Results for the standard curves are consistent with previous studies that had documented that $R^2 > 0.99$ indicates highly reproducible and reliable qPCR assays for bacterial and viral systems (Gentle, Anastasopoulos, & McBrien, 2001; Ruijter et al., 2009). This linearity is consistent across all experimental conditions and demonstrates the quantitation capability of the assay under any DNA integrity or sample source (Tellinghuisen & Spiess, 2014). Uniformity of standard curve performance for the different MABC subspecies also indicates resilience to minor fluctuations in DNA fragmentation and matrix variability.

4.3.2 Amplification Efficiency

Amplification efficiency in qPCR is closely linked to the integrity of the template DNA. In cfDNA, which is often fragmented due to processes like apoptosis and necrosis, the DNA strands can have breaks and damaged ends. These fragments make it harder for primers to bind properly and for the polymerase to extend the new sandwich reduce the overall efficiency of amplification (Terp, Pedersen, & Stoico, 2024). This is a common issue in cfDNA research, especially when trying to amplify DNA regions that are longer than the average fragment size. In this research, Primer Set 6 exhibited excellent amplification efficiency (93–104%) when used on intact genomic DNA under ideal conditions and proved suitable according to our requirements. However, when used on enzymatically fragmented cfDNA simulants, efficiency decreased to around 87%, as also previously reported by (Lai et al., 2023) fragmentation may produce overhangs or nicked duplexes that interfere with Taq polymerase efficacy, as reported by studies analysing severely fragmented viral and tumor cfDNA templates. The efficiency in plasma matrix conditions declined for Maa and Mam (~87%) but remained relatively stable for Mab (up to 101%). This trend can be explained by the combined effects of DNA fragmentation and plasma matrix interference. Plasma contains inhibitors such as immunoglobulins, heme, and residual EDTA, which are known to interfere with qPCR amplification (Schrader et al., 2012). Additionally, cfDNA recovery can vary across subspecies due to differences in fragment size distribution, methylation patterns and extraction efficiency (Devonshire et al., 2014). For example, Maa may have produced shorter or more degraded fragments that were less efficiently recovered or amplified, accounting for the observed drop in efficiency. Similar differential extraction and amplification performance has been described by (Rather, 2024) in the context of cfDNA from fetal versus maternal sources.

4.3.3 Limit of detection

cfDNA is typically found in low concentrations in the bloodstream and exists in a highly fragmented state, making it a challenging analyte for molecular detection. Inaccurate or inadequate sensitivity can result in false-negative results. In this study with optimal conditions using unfragmented genomic DNA, Primer Set 6 had exceptionally low LODs (~1 copy/µL for all MABC subspecies) **(Table 3.5)**, which is consistent with existing published work showing that high-integrity templates support strong amplification even at very low input concentrations (Svec et al., 2015). These low LODs are due to complete amplicons being available for efficient binding and extension during PCR, enabling polymerase to produce full-length products with lower Ct values (Forootan et al., 2017). After enzymatic fragmentation, noticed a modest but significant increase in LOD **(Figure 3.6)**. This is consistent with studies like those by (Sedlackova et al., 2013) and (Swango et al., 2006) which indicate that strand breakage of DNA lowers the availability for amplification of intact target sequences. Even when it binds to a primer, a damaged amplicon can block complete extension, leading to increased Ct values and decreased sensitivity (Sedlackova et al., 2013). In mock plasma cfDNA conditions, LODs rose further ~20 copies/µL **(Figure 3.7)**, demonstrating further biological and technical issues. These are matrix interference caused by plasma components (e.g., proteins, haemoglobin, EDTA), which have been shown to reduce polymerase activity (Schrader et al., 2012), and incomplete recovery of cfDNA throughout extraction, particularly at low input yields. (Barrett et al., 2020; Devonshire et al., 2014; Terp, Pedersen, & Stoico, 2024) reported varying yields for cfDNA between genomic loci and between sample types, leading to uneven recovery and effective input to downstream amplification. Despite these challenges, the LODs for all three subspecies remained within clinically acceptable ranges, based on previously reported cfDNA concentrations in the blood of *Mycobacterium tuberculosis* patients, which ranged from 0.74 copies/µL (median) to a mean of 7.20 ± 29.15 copies/µL (Huang et al., 2022). This assay was designed with a target LOD of < 50 copies/µL of extraction to ensure diagnostic applicability. However, sensitivity may decline as the complexity of biology increases, but Primer Set 6 maintains clinical relevance and practical utility, particularly in low-template scenarios such as early-stage infections and post-treatment monitoring.

4.4 Reproducibility analysis of Primer set 6.

Ensuring assay reproducibility is essential for the translation of molecular diagnostics into clinical settings particularly in detecting low abundance cfDNA in plasma. Reproducibility reflects not only the technical robustness of the qPCR assay but also the reliability across different conditions, operators, and instruments. As emphasised in the prior digital PCR studies (Wang et al., 2024) (Blauwkamp et al., 2019) high reproducibility becomes critical when monitoring small changes in cfDNA abundance across different time points or in different clinical cohorts. Fragmented DNA yields a homogeneous and quantifiably controlled template that allows reproducibility measures like Ct values, coefficient variation (CV%), and standard curve slopes to reflect fidelity of the assay and not pre-analytical variation. Therefore, assessing reproducibility using fragmented DNA offers a more accurate reflection of the assay's real-world performance, especially in the context of detecting low-abundance MABC cfDNA in plasma from pwCF.

4.4.1 Intra assay reproducibility

In this research intra-assay reproducibility was examined by three technical replicates (CT1, CT2, CT3) of serially diluted fragmented DNA **(Figure 3.7A-B)**. Ct values showed high agreement between replicates, notably at mid-to-high DNA concentrations, with little variance. As expected, variability increased at concentrations near the assay's LOD. This pattern is due to increased random fluctuation of amplification caused by the small number of target molecules in the reaction. This is a situation in which, in certain replicates, there is a single target copy that is successfully amplified, whereas in others, the target is absent or inappropriately amplified by random sampling effects (Pan et al., 2010). This is due to the inherent Poisson distribution effect in pipetting and molecular partitioning; when the average number of template copies per reaction (close to 1–3 copies), random chance alone determines whether sufficient intact targets are included in each of the reaction wells. Even slight pipetting error, or partial degradation of a fragment, can result in delayed or undetectable amplification (Pandya et al., 2010). However, (Guan et al., 2023) reported in qPCR literature that precision of analysis is decreased as the concentration of the template gets closer to the limit of detection, resulting in increased standard deviations and lowered repeatability. These findings affirm that Primer Set 6 performs reliably in typical diagnostic ranges, with only expected variability near detection thresholds.

4.4.2 Inter assay reproducibility.

The inter-assay reproducibility of Primer Set 6 was tested under three independent runs of qPCR, and the findings confirm high levels of analytical reproducibility and stability. In this research CV% of slope and Ct values at high and low template concentrations were calculated and found to be less than 3%, above reproducibility standards as established by the MIQE guidelines recommending CV <5% for high-quality qPCR optimization (Bustin et al., 2009). This low CV between assays is essential for diagnostics where decision-making can be predicated upon small changes in target amount in cfDNA-based infectious disease monitoring and treatment response assessment. Similar levels of reproducibility have been reported in the literature. (Kubista et al., 2006) highlighted the need for generating reproducible standard curves and slope values for reliable quantitative performance. Similarly, (Kubista et al., 2006) highlighted that assays used for clinical or high-sensitivity applications must demonstrate reproducibility across multiple runs to be considered diagnostically viable. The performance of Primer Set 6 is in line with these requirements and shows suitability for wider-scale clinical processes such as tracking circulating MABC cfDNA in patients over time.

4.5 Research Gaps and Future Directions.

4.5.1 Limitations in current qPCR and CRISPR applications

Pathogen detection has been revolutionized using molecular diagnostics to achieve fast, sensitive, and specific analysis versus the traditional microbiological methods. qPCR and CRISPR-based platforms are two significant tools in this regard when it comes to microbiological surveillance in complicated cases such as NTM infections. Both technologies, however promising they are, possess distinct limitations which are worthy of critical consideration, especially in the current study.

One significant constraint in the current work was the inability to experimentally prove the CRISPR-Cas12a based specificity enhancement strategy which were incorporated conceptually. This system was designed to enhance post-amplification specificity through the use of targeted gRNA, aiming to eliminate off-target cross-reactivity in the case of conserved genes such as 23S rRNA, which was the target in Primer 6. However, due to time and resource limitations, this aspect was not experimentally tested. Existing research (Li et al., 2024), validates the high potential of Cas12a in the reduction of false-positive signals by way of

collateral cleavage-based fluorescence, the implementation of which needs to take place in the future.

In addition, the third objective of this project, clinical validation of the qPCR assay with cfDNA from individuals with cystic fibrosis (pwCF) was left unfinished. Lack of time to go through the CRISPR based enhancement and logistical delays prevented this key stage from being achieved. This is an essential step for establishing key diagnostic parameters including sensitivity, specificity in real world performance using the clinical samples. Without this stage, the actual clinical utility of the assay is yet to be fully defined. In spite of the limitations mentioned, both the technologies are vital diagnostic tools. Their combination qPCR as an initial quantification and CRISPR for downstream verification is a pathway towards extremely accurate and less-invasive testing platforms for the detection of MABC cfDNA in at-risk groups such as pwCF. However, full diagnostic implementation will depend on overcoming current validation berries via subsequent studies and clinical translation.

4.5.2 Future molecular diagnostic methods in MABC infection

The landscape of molecular diagnostics is rapidly evolving towards faster, more sensitive, and minimally invasive approaches. Molecular diagnostic methods are a crucial advancement in infection disease diagnostics because conventional diagnostic methods underperformed or less accurate. This is especially true for vulnerable populations like pwCF in whom obtaining high-quality respiratory samples can be challenging. In this context, non-invasive biomarker strategies particularly the analysis of cfDNA in MABC infection are emerging as valuable tools for providing real-time, systemic insights into infection status and progression.

Future efforts should focus on completing the CRISPR-Cas12a integration for specificity and sensitivity enhancement and progressing toward comprehensive clinical validation using cfDNA extracted from the plasma of pwCF. Furthermore, development of diagnostic tools based on the CRISPR technique, such as the ERA-CRISPR/Cas12 system (Deng et al., 2022), opens new perspectives for rapid and precise diagnostics. The technique does not need complex thermal cycling, which offers the possibility of obtaining results in less than one hour, promising for point-of-care applications (Ali et al., 2023). CRISPR-based assays are highly suited for MABC detection, given their ability to distinguish between closely related subspecies and detect low bacterial loads in clinical specimens (Sahoo, Jadhav, & Nema, 2024).

Moreover, the combination of CRISPR with isothermal amplification, as seen in ERA, has further improved the speed and accuracy that could become a game-changing tool in the diagnosis of MABC. One of the novel areas researched includes the cfDNA present in the blood

as a diagnostic marker for MABC infection. This less invasive approach offers a promising alternative to traditional sputum-based diagnostics. Studies have demonstrated the potential of cfDNA in the diagnosis of Mycobacterial infections, including the detection of MAC infections using CRISPR-based assays. This technology enables the detection of microbial cfDNA in serum with high sensitivity and specificity, providing a rapid diagnostic tool that could significantly improve the management of MABC infections (Li et al., 2024). Additionally, cfDNA could be used to monitor treatment effectiveness in real time by tracking the levels of bacterial DNA during therapy.

Looking forward, this would probably integrate Next Generation Sequencing (NGS) with CRISPR-based diagnostics in the future to provide a more holistic approach to MABC detection and its resistance patterns (Chakraborty et al., 2022). The combination of NGS and CRISPR could also aid in the rapid identification of novel resistance mechanisms in MABC, a critical factor for managing the notorious drug-resistant pathogens. Future developments of microfluidics and lab-on-a-chip technologies may allow for the miniaturization of CRISPR diagnostics, hence offering applications in point-of-care settings and resource-limited environments.

4.6 Conclusion

In conclusion, this study lays a strong foundation for the development of a cfDNA based molecular diagnostic platform for detecting MABC in pwCF. The PCR assay using Primer set 6 showed excellent sensitivity and reproducibility in a controlled setting. However, CRISPR integration for increasing the specificity and sensitivity of the assay remains as a future goal. The findings support continued development of this assay as a promising alternative to traditional respiratory bacterial diagnostics, with potential application in early detection, treatment monitoring and improved patient care.

Bibliography

Akwani, W. C., van Vliet, A. H. M., Joel, J. O., Andres, S., Diricks, M., Maurer, F. P., Chambers, M. A., & Hingley-Wilson, S. M. (2022). The Use of Comparative Genomic Analysis for the Development of Subspecies-Specific PCR Assays for Mycobacterium abscessus. *Front Cell Infect Microbiol*, *12*, 816615. https://doi.org/10.3389/fcimb.2022.816615

Ali, A., Zafar, M. M., Farooq, Z., Ahmed, S. R., Ijaz, A., Anwar, Z., Abbas, H., Tariq, M. S., Tariq, H., Mustafa, M., Bajwa, M. H., Shaukat, F., Razzaq, A., & Maozhi, R. (2023). Breakthrough in CRISPR/Cas system: Current and future directions and challenges. *Biotechnol J*, *18*(8), e2200642. https://doi.org/10.1002/biot.202200642

Bar-On, O., Mussaffi, H., Mei-Zahav, M., Prais, D., Steuer, G., Stafler, P., Hananya, S., & Blau, H. (2015). Increasing nontuberculous mycobacteria infection in cystic fibrosis. *J Cyst Fibros*, *14*(1), 53-62. https://doi.org/10.1016/j.jcf.2014.05.008

Barrett, S. L. R., Holmes, E. A., Long, D. R., Shean, R. C., Bautista, G. E., Ravishankar, S., Peddu, V., Cookson, B. T., Singh, P. K., & Greninger, A. L. (2020). Cell free DNA from respiratory pathogens is detectable in the blood plasma of cystic fibrosis patients. *Scientific Reports*, *10*(1), 6903. https://doi.org/ https://doi.org/10.1038/s41598-020-63970-0

Bensi, E. P., Panunto, P. C., & Ramos Mde, C. (2013). Incidence of tuberculous and non-tuberculous mycobacteria, differentiated by multiplex PCR, in clinical specimens of a large general hospital. *Clinics (Sao Paulo)*, *68*(2), 179-184. https://doi.org/10.6061/clinics/2013(02)oa10

Blauwkamp, T. A., Thair, S., Rosen, M. J., Blair, L., Lindner, M. S., Vilfan, I. D., Kawli, T., Christians, F. C., Venkatasubrahmanyam, S., Wall, G. D., Cheung, A., Rogers, Z. N., Meshulam-Simon, G., Huijse, L., Balakrishnan, S., Quinn, J. V., Hollemon, D., Hong, D. K., Vaughn, M. L., . . . Yang, S. (2019). Analytical and clinical validation of a microbial cell-free DNA sequencing test for infectious disease. *Nat Microbiol*, *4*(4), 663-674. https://doi.org/10.1038/s41564-018-0349-6

Burnham, P., Dadhania, D., Heyang, M., Chen, F., Westblade, L. F., Suthanthiran, M., Lee, J. R., & De Vlaminck, I. (2018). Urinary cell-free DNA is a versatile analyte for monitoring infections of the urinary tract. *Nature communications*, *9*(1), 2412. https://doi.org/https://doi.org/10.1038/s41467-018-04745-0

Bustin, S. A., Benes, V., Garson, J. A., Hellemans, J., Huggett, J., Kubista, M., Mueller, R., Nolan, T., Pfaffl, M. W., & Shipley, G. L. (2009). The MIQE Guidelines: M inimum I nformation for Publication of Q uantitative Real-Time PCR E xperiments. In: Oxford University Press.

Chakraborty, J., Chaudhary, A. A., Khan, S. U., Rudayni, H. A., Rahaman, S. M., & Sarkar, H. (2022). CRISPR/Cas-Based Biosensor As a New Age Detection Method for Pathogenic Bacteria. *ACS omega*, *7*(44), 39562-39573. https://doi.org/10.1021/acsomega.2c04513

Chen, L.-T., Wesdorp, E., Jager, M., Siegers, E. W., Theelen, M. J., Besselink, N., Vermeulen, C., Zomer, A. L., Broens, E. M., & Wagenaar, J. A. (2024). Bacterial cell-free DNA profiling reveals co-elevation of multiple bacteria in newborn foals with suspected sepsis. *bioRxiv*, 2024.2010. 2031.620104. https://doi.org/https://doi.org/10.1101/2024.10.31.620104

Chen, Y., Wu, S., Wu, H., Cheng, P., Wang, X., Qian, S., Zhang, M., Xu, J., Ji, F., & Wu, J. (2021). CRISPR/Cas12a-Based Versatile Method for Checking Quantitative Polymerase Chain Reaction Samples with Cycles of Threshold Values in the Gray Zone. *ACS Sens*, *6*(5), 1963-1970. https://doi.org/10.1021/acssensors.1c00515

Cho, Y.-J., Yi, H., Chun, J., Cho, S.-N., Daley, C. L., Koh, W.-J., & Jae Shin, S. (2013). The genome sequence of 'Mycobacterium massiliense'strain CIP 108297 suggests the independent taxonomic status of the Mycobacterium abscessus complex at the subspecies level. *PLoS One*, *8*(11), e81560. https://doi.org/https://doi.org/10.1371/journal.pone.0081560

Choi, G. E., Chang, C. L., Whang, J., Kim, H. J., Kwon, O. J., Koh, W. J., & Shin, S. J. (2011). Efficient differentiation of Mycobacterium abscessus complex isolates to the species level by a novel PCR-based variable-number tandem-repeat assay. *J Clin Microbiol*, *49*(3), 1107-1109. https://doi.org/10.1128/JCM.02318-10

Davidson, R. M., Benoit, J. B., Kammlade, S. M., Hasan, N. A., Epperson, L. E., Smith, T., Vasireddy, S., Brown-Elliott, B. A., Nick, J. A., Olivier, K. N., Zelazny, A. M., Daley, C. L., Strong, M., & Wallace, R. J., Jr. (2021). Genomic characterization of sporadic isolates of the dominant clone of Mycobacterium abscessus subspecies massiliense. *Sci Rep*, *11*(1), 15336. https://doi.org/10.1038/s41598-021-94789-y

Deng, Z., Hu, H., Tang, D., Liang, J., Su, X., Jiang, T., Hu, X., Ying, W., Zhen, D., & Xiao, X. (2022). Ultrasensitive, Specific, and Rapid Detection of Mycoplasma pneumoniae

Using the ERA/CRISPR–Cas12a Dual System. *Frontiers in Microbiology*, *13*, 811768. https://doi.org/https://doi.org/10.3389/fmicb.2022.811768

Devonshire, A. S., Whale, A. S., Gutteridge, A., Jones, G., Cowen, S., Foy, C. A., & Huggett, J. F. (2014). Towards standardisation of cell-free DNA measurement in plasma: controls for extraction efficiency, fragment size bias and quantification. *Anal Bioanal Chem*, *406*(26), 6499-6512. https://doi.org/10.1007/s00216-014-7835-3

Dziedzinska, R., Okunkova, J., Kralik, P., Svobodova, J., Mala, M., & Slana, I. (2022a). Identification of and discrimination between the

complex and

complex directly from sputum using quadruplex real-time PCR. *Journal of Medical Microbiology*, *71*(12), 001611. https://doi.org/ARTN 001611

10.1099/jmm.0.001611

Dziedzinska, R., Okunkova, J., Kralik, P., Svobodova, J., Mala, M., & Slana, I. (2022b). Identification of and discrimination between the Mycobacterium abscessus complex and Mycobacterium avium complex directly from sputum using quadruplex real-time PCR. *J Med Microbiol*, *71*(12), 001611. https://doi.org/10.1099/jmm.0.001611

Evans, I., Weimann, A., Baird, T., Haworth, C., & Floto, A. (2025). Mycobacterium abscessus treatment outcomes in cystic fibrosis: A single centre experience. *J Cyst Fibros*, *24*(2), 364-367. https://doi.org/10.1016/j.jcf.2024.07.016

Fairhurst, R. M., Kubak, B. M., Shpiner, R. B., Levine, M. S., Pegues, D. A., & Ardehali, A. (2002). Mycobacterium abscessus empyema in a lung transplant recipient. *J Heart Lung Transplant*, *21*(3), 391-394. https://doi.org/10.1016/s1053-2498(01)00339-4

Forootan, A., Sjoback, R., Bjorkman, J., Sjogreen, B., Linz, L., & Kubista, M. (2017). Methods to determine limit of detection and limit of quantification in quantitative real-time PCR (qPCR). *Biomol Detect Quantif*, *12*, 1-6. https://doi.org/10.1016/j.bdq.2017.04.001

Forton, J. (2015). Induced sputum in young healthy children with cystic fibrosis. *Paediatr Respir Rev*, *16 Suppl 1*, 6-8. https://doi.org/10.1016/j.prrv.2015.07.007

Fredman, D., Jobs, M., Strömqvist, L., & Brookes, A. (2004). DFold: PCR design that minimizes secondary structure and optimizes downstream genotyping applications. *Human mutation*, *24*(1), 1-8. https://doi.org/https://doi.org/10.1002/humu.20066

Gan, T., Yu, J., Deng, Z., & He, J. (2024). ERA-CRISPR/Cas12a system: a rapid, highly sensitive and specific assay for Mycobacterium tuberculosis. *Front Cell Infect Microbiol*, *14*, 1454076. https://doi.org/10.3389/fcimb.2024.1454076

Garrison, A. P., Morris, M. I., Doblecki Lewis, S., Smith, L., Cleary, T. J., Procop, G. W., Vincek, V., Rosa-Cunha, I., Alfonso, B., Burke, G. W., Tzakis, A., & Hartstein, A. I. (2009). Mycobacterium abscessus infection in solid organ transplant recipients: report of three cases and review of the literature. *Transpl Infect Dis*, *11*(6), 541-548. https://doi.org/10.1111/j.1399-3062.2009.00434.x

Gentle, A., Anastasopoulos, F., & McBrien, N. A. (2001). High-resolution semi-quantitative real-time PCR without the use of a standard curve. *Biotechniques*, *31*(3), 502-508. https://doi.org/https://doi.org/10.2144/01313st03

Goethe, R., Laarmann, K., Sproer, C., & Bunk, B. (2020). Complete Genome Sequence of Mycobacterium avium subsp. avium Chester (DSM 44156). *Microbiol Resour Announc*, *9*(7), 10.1128/mra. 01549-01519. https://doi.org/10.1128/MRA.01549-19

Guan, X. L., Chang, D. P. S., Mok, Z. X., & Lee, B. (2023). Assessing variations in manual pipetting: An under-investigated requirement of good laboratory practice. *J Mass Spectrom Adv Clin Lab*, *30*, 25-29. https://doi.org/10.1016/j.jmsacl.2023.09.001

Guion, C. E., Ochoa, T. J., Walker, C. M., Barletta, F., & Cleary, T. G. (2008). Detection of diarrheagenic Escherichia coli by use of melting-curve analysis and real-time multiplex PCR. *J Clin Microbiol*, *46*(5), 1752-1757. https://doi.org/10.1128/JCM.02341-07

Harun, S. N., Wainwright, C., Klein, K., & Hennig, S. (2016). A systematic review of studies examining the rate of lung function decline in patients with cystic fibrosis. *Paediatr Respir Rev*, *20*, 55-66. https://doi.org/10.1016/j.prrv.2016.03.002

Hu, Y., Zhao, Y., Zhang, Y., Chen, W., Zhang, H., & Jin, X. (2025). Cell-free DNA: a promising biomarker in infectious diseases. *Trends Microbiol*, *33*(4), 421-433. https://doi.org/10.1016/j.tim.2024.06.005

Huang, Z., LaCourse, S. M., Kay, A. W., Stern, J., Escudero, J. N., Youngquist, B. M., Zheng, W., Vambe, D., Dlamini, M., Mtetwa, G., Cranmer, L. M., Njuguna, I., Wamalwa, D. C., Maleche-Obimbo, E., Catanzaro, D. G., Lyon, C. J., John-Stewart, G., DiNardo, A., Mandalakas, A. M., . . . Hu, T. Y. (2022). CRISPR detection of circulating cell-free Mycobacterium tuberculosis DNA in adults and children, including children with HIV: a molecular diagnostics study. *Lancet Microbe*, *3*(7), e482-e492. https://doi.org/10.1016/S2666-5247(22)00087-8

Huttunen, R., Kuparinen, T., Jylhävä, J., Aittoniemi, J., Vuento, R., Huhtala, H., Laine, J., Syrjänen, J., & Hurme, M. (2011). Fatal outcome in bacteremia is characterized by high plasma cell free DNA concentration and apoptotic DNA fragmentation: a

prospective cohort study. *PLoS One*, *6*(7), e21700. https://doi.org/https://doi.org/10.1371/journal.pone.0021700

Integrated DNA Technologies, I. *OligoAnalyzer Tool*.

Jaen-Luchoro, D., Salva-Serra, F., Aliaga-Lozano, F., Segui, C., Busquets, A., Ramirez, A., Ruiz, M., Gomila, M., Lalucat, J., & Bennasar-Figueras, A. (2016). Complete Genome Sequence of Mycobacterium chelonae Type Strain CCUG 47445, a Rapidly Growing Species of Nontuberculous Mycobacteria. *Genome Announc*, *4*(3), 10.1128/genomea. 00550-00516. https://doi.org/10.1128/genomeA.00550-16

Jeon, K., Kwon, O. J., Lee, N. Y., Kim, B. J., Kook, Y. H., Lee, S. H., Park, Y. K., Kim, C. K., & Koh, W. J. (2009). Antibiotic treatment of Mycobacterium abscessus lung disease: a retrospective analysis of 65 patients. *Am J Respir Crit Care Med*, *180*(9), 896-902. https://doi.org/10.1164/rccm.200905-0704OC

Jeong, B. H., Kim, S. Y., Jeon, K., Lee, S. Y., Shin, S. J., & Koh, W. J. (2013). Serodiagnosis of Mycobacterium avium complex and Mycobacterium abscessus complex pulmonary disease by use of IgA antibodies to glycopeptidolipid core antigen. *J Clin Microbiol*, *51*(8), 2747-2749. https://doi.org/10.1128/JCM.00702-13

Johansen, M. D., Herrmann, J. L., & Kremer, L. (2020). Non-tuberculous mycobacteria and the rise of Mycobacterium abscessus. *Nat Rev Microbiol*, *18*(7), 392-407. https://doi.org/10.1038/s41579-020-0331-1

Johnston, A. D., Lu, J., Ru, K. L., Korbie, D., & Trau, M. (2019). PrimerROC: accurate condition-independent dimer prediction using ROC analysis. *Sci Rep*, *9*(1), 209. https://doi.org/10.1038/s41598-018-36612-9

Jonsson, B. E., Gilljam, M., Lindblad, A., Ridell, M., Wold, A. E., & Welinder-Olsson, C. (2007). Molecular epidemiology of Mycobacterium abscessus, with focus on cystic fibrosis. *J Clin Microbiol*, *45*(5), 1497-1504. https://doi.org/10.1128/JCM.02592-06

Kim, B.-J., Choi, B.-S., Lim, J.-S., Choi, I.-Y., Lee, J.-H., Chun, J., Kook, Y.-H., & Kim, B.-J. (2012). Complete genome sequence of Mycobacterium intracellulare strain ATCC 13950T. In: American Society for Microbiology 1752 N St., NW, Washington, DC.

Kim, K., Hong, S. H., Kim, B. J., Kim, B. R., Lee, S. Y., Kim, G. N., Shim, T. S., Kook, Y. H., & Kim, B. J. (2015). Separation of Mycobacterium abscessus into subspecies or genotype level by direct application of peptide nucleic acid multi-probe- real-time PCR method into sputa samples. *BMC Infect Dis*, *15*, 325. https://doi.org/10.1186/s12879-015-1076-8

Koehler, D. R., Sajjan, U., Chow, Y. H., Martin, B., Kent, G., Tanswell, A. K., McKerlie, C., Forstner, J. F., & Hu, J. (2003). Protection of Cftr knockout mice from acute lung infection by a helper-dependent adenoviral vector expressing Cftr in airway epithelia. *Proc Natl Acad Sci U S A*, *100*(26), 15364-15369. https://doi.org/10.1073/pnas.2436478100

Koh, W. J., Jeong, B. H., Kim, S. Y., Jeon, K., Park, K. U., Jhun, B. W., Lee, H., Park, H. Y., Kim, D. H., Huh, H. J., Ki, C. S., Lee, N. Y., Kim, H. K., Choi, Y. S., Kim, J., Lee, S. H., Kim, C. K., Shin, S. J., Daley, C. L., . . . Kwon, O. J. (2017). Mycobacterial Characteristics and Treatment Outcomes in Mycobacterium abscessus Lung Disease. *Clin Infect Dis*, *64*(3), 309-316. https://doi.org/10.1093/cid/ciw724

Koskinen, M. T., Holopainen, J., Pyorala, S., Bredbacka, P., Pitkala, A., Barkema, H. W., Bexiga, R., Roberson, J., Solverod, L., Piccinini, R., Kelton, D., Lehmusto, H., Niskala, S., & Salmikivi, L. (2009). Analytical specificity and sensitivity of a real-time polymerase chain reaction assay for identification of bovine mastitis pathogens. *J Dairy Sci*, *92*(3), 952-959. https://doi.org/10.3168/jds.2008-1549

Kubista, M., Andrade, J. M., Bengtsson, M., Forootan, A., Jonak, J., Lind, K., Sindelka, R., Sjoback, R., Sjogreen, B., Strombom, L., Stahlberg, A., & Zoric, N. (2006). The real-time polymerase chain reaction. *Mol Aspects Med*, *27*(2-3), 95-125. https://doi.org/10.1016/j.mam.2005.12.007

Lai, C. H., Lin, Y. S., Wang, C. M., Chang, P. C., & Shia, W. Y. (2023). A Novel 16S rRNA PCR-Restriction Fragment Length Polymorphism Assay to Accurately Distinguish Zoonotic Capnocytophaga canimorsus and C. cynodegmi. *Microbiol Spectr*, *11*(3), e0291622. https://doi.org/10.1128/spectrum.02916-22

Lavie, M., Manovitz, T., Vilozni, D., Levy-Mendelovich, S., Sarouk, I., Weintraubv, I., Shoseyov, D., Cohen-Cymberknoh, M., Rivlin, J., & Efrati, O. (2015). Long-term follow-up of distal intestinal obstruction syndrome in cystic fibrosis. *World J Gastroenterol*, *21*(1), 318-325. https://doi.org/10.3748/wjg.v21.i1.318

Lee, M. R., Sheng, W. H., Hung, C. C., Yu, C. J., Lee, L. N., & Hsueh, P. R. (2015). Mycobacterium abscessus Complex Infections in Humans. *Emerg Infect Dis*, *21*(9), 1638-1646. https://doi.org/10.3201/2109.141634

Li, L., Henkle, E., Youngquist, B. M., Seo, S., Hamed, K., Melnick, D., Lyon, C. J., Jiang, L., Zelazny, A. M., Hu, T. Y., Winthrop, K. L., & Ning, B. (2024). Serum Cell-Free DNA-based Detection of Mycobacterium avium Complex Infection. *Am J Respir Crit Care Med*, *209*(10), 1246-1254. https://doi.org/10.1164/rccm.202303-0401OC

Liu, C. F., Song, Y. M., He, W. C., Liu, D. X., He, P., Bao, J. J., Wang, X. Y., Li, Y. M., & Zhao, Y. L. (2021). Nontuberculous mycobacteria in China: incidence and antimicrobial resistance spectrum from a nationwide survey. *Infect Dis Poverty*, *10*(1), 59. https://doi.org/10.1186/s40249-021-00844-1

Long, D. R., Holmes, E. A., Goss, C. H., Singh, P. K., Waalkes, A., & Salipante, S. J. (2023). Cell-Free DNA Detects Pseudomonas aeruginosa Lung Infection in Modulator-treated People with Cystic Fibrosis. *Am J Respir Crit Care Med*, *208*(9), 944-947. https://doi.org/10.1164/rccm.202305-0844LE

Lopez-Roa, P., Esteban, J., & Munoz-Egea, M. C. (2022). Updated Review on the Mechanisms of Pathogenicity in Mycobacterium abscessus, a Rapidly Growing Emerging Pathogen. *Microorganisms*, *11*(1), 90. https://doi.org/10.3390/microorganisms11010090

Macheras, E., Roux, A. L., Ripoll, F., Sivadon-Tardy, V., Gutierrez, C., Gaillard, J. L., & Heym, B. (2009). Inaccuracy of single-target sequencing for discriminating species of the Mycobacterium abscessus group. *J Clin Microbiol*, *47*(8), 2596-2600. https://doi.org/10.1128/JCM.00037-09

Malhotra, S., Hayes, D., Jr., & Wozniak, D. J. (2019). Cystic Fibrosis and Pseudomonas aeruginosa: the Host-Microbe Interface. *Clin Microbiol Rev*, *32*(3), 10.1128/cmr. 00138-00118. https://doi.org/10.1128/CMR.00138-18

Mandel, P. (1948). Les acides nucleiques du plasma sanguin chez 1 homme. *CR Seances Soc Biol Fil*, *142*, 241-243.

Marshall, J. E., Mercaldo, R. A., Lipner, E. M., & Prevots, D. R. (2023). Incidence of nontuberculous mycobacteria infections among persons with cystic fibrosis in the United States (2010-2019). *BMC Infect Dis*, *23*(1), 489. https://doi.org/10.1186/s12879-023-08468-6

Nakanaga, K., Sekizuka, T., Fukano, H., Sakakibara, Y., Takeuchi, F., Wada, S., Ishii, N., Makino, M., Kuroda, M., & Hoshino, Y. (2014). Discrimination of Mycobacterium abscessus subsp. massiliense from Mycobacterium abscessus subsp. abscessus in clinical isolates by multiplex PCR. *J Clin Microbiol*, *52*(1), 251-259. https://doi.org/10.1128/JCM.01327-13

Nash, K. A., Brown-Elliott, B. A., & Wallace, R. J., Jr. (2009). A novel gene, erm(41), confers inducible macrolide resistance to clinical isolates of Mycobacterium abscessus but is absent from Mycobacterium chelonae. *Antimicrob Agents Chemother*, *53*(4), 1367-1376. https://doi.org/10.1128/AAC.01275-08

Novosad, S. A., Beekmann, S. E., Polgreen, P. M., Mackey, K., Winthrop, K. L., & Team, M. a. S. (2016). Treatment of Mycobacterium abscessus Infection. *Emerg Infect Dis*, *22*(3), 511-514. https://doi.org/10.3201/eid2203.150828

Pagin, A., Sermet-Gaudelus, I., & Burgel, P. R. (2020). Genetic diagnosis in practice: From cystic fibrosis to CFTR-related disorders. *Arch Pediatr*, *27 Suppl 1*, eS25-eS29. https://doi.org/10.1016/S0929-693X(20)30047-6

Pan, Y., Bodrossy, L., Frenzel, P., Hestnes, A. G., Krause, S., Luke, C., Meima-Franke, M., Siljanen, H., Svenning, M. M., & Bodelier, P. L. (2010). Impacts of inter- and intralaboratory variations on the reproducibility of microbial community analyses. *Appl Environ Microbiol*, *76*(22), 7451-7458. https://doi.org/10.1128/AEM.01595-10

Panda, A., Nagaraj, S., Zhao, X., Tettelin, H., & DeTolla, L. J. (2017). Complete Genome Sequences of Mycobacterium kansasii Strains Isolated from Rhesus Macaques. *Genome Announc*, *5*(16), 10.1128/genomea. 00187-00117. https://doi.org/10.1128/genomeA.00187-17

Pandya, K., Ray, C. A., Brunner, L., Wang, J., Lee, J. W., & DeSilva, B. (2010). Strategies to minimize variability and bias associated with manual pipetting in ligand binding assays to assure data quality of protein therapeutic quantification. *Journal of pharmaceutical and biomedical analysis*, *53*(3), 623-630. https://doi.org/https://doi.org/10.1016/j.jpba.2010.04.025

Park, I. K., Hsu, A. P., Tettelin, H., Shallom, S. J., Drake, S. K., Ding, L., Wu, U. I., Adamo, N., Prevots, D. R., Olivier, K. N., Holland, S. M., Sampaio, E. P., & Zelazny, A. M. (2015). Clonal Diversification and Changes in Lipid Traits and Colony Morphology in Mycobacterium abscessus Clinical Isolates. *J Clin Microbiol*, *53*(11), 3438-3447. https://doi.org/10.1128/JCM.02015-15

Park, J. H., Koo, B., Kim, M. J., Lee, H. J., Cha, H. H., Kim, J. Y., Lee, S. W., Shin, Y., & Kim, S. H. (2022). Utility of plasma cell-free DNA detection using homobifunctional imidoesters using a microfluidic system for diagnosing active tuberculosis. *Infect Dis (Lond)*, *54*(1), 46-52. https://doi.org/10.1080/23744235.2021.1963839

Pietrzak, B., Kawacka, I., Olejnik-Schmidt, A., & Schmidt, M. (2023). Circulating Microbial Cell-Free DNA in Health and Disease. *Int J Mol Sci*, *24*(3), 3051. https://doi.org/10.3390/ijms24033051

Pollock, N. R., MacIntyre, A. T., Blauwkamp, T. A., Blair, L., Ho, C., Calderon, R., & Franke, M. F. (2021). Detection of Mycobacterium tuberculosis cell-free DNA to

diagnose TB in pediatric and adult patients. *Int J Tuberc Lung Dis*, *25*(5), 403-405. https://doi.org/10.5588/ijtld.21.0055

Preece, C. L., Wichelhaus, T. A., Perry, A., Jones, A. L., Cummings, S. P., Perry, J. D., & Hogardt, M. (2016). Evaluation of Various Culture Media for Detection of Rapidly Growing Mycobacteria from Patients with Cystic Fibrosis. *J Clin Microbiol*, *54*(7), 1797-1803. https://doi.org/10.1128/JCM.00471-16

Rahimi, H., Salehiabar, M., Barsbay, M., Ghaffarlou, M., Kavetskyy, T., Sharafi, A., Davaran, S., Chauhan, S. C., Danafar, H., Kaboli, S., Nosrati, H., Yallapu, M. M., & Conde, J. (2021). CRISPR Systems for COVID-19 Diagnosis. *ACS Sens*, *6*(4), 1430-1445. https://doi.org/10.1021/acssensors.0c02312

Ramananda, Y., Naren, A. P., & Arora, K. (2024). Functional Consequences of CFTR Interactions in Cystic Fibrosis. *Int J Mol Sci*, *25*(6), 3384. https://doi.org/10.3390/ijms25063384

Rather, R. A. (2024). Fetal Origin Circulating Cell-Free Nucleic Acids in Maternal Circulation and Their Clinical Importance. In *Non-invasive Prenatal Screening (NIPS) in Clinical Practice* (pp. 17-35). Springer. https://doi.org/https://doi.org/10.1007/978-981-97-6402-0_2

Recchia, D., Stelitano, G., Stamilla, A., Gutierrez, D. L., Degiacomi, G., Chiarelli, L. R., & Pasca, M. R. (2023). Mycobacterium abscessus Infections in Cystic Fibrosis Individuals: A Review on Therapeutic Options. *Int J Mol Sci*, *24*(5), 4635. https://doi.org/10.3390/ijms24054635

Rodriguez-Temporal, D., Herrera, L., Alcaide, F., Domingo, D., Hery-Arnaud, G., van Ingen, J., Van den Bossche, A., Ingebretsen, A., Beauruelle, C., Terschlusen, E., Boarbi, S., Vila, N., Arroyo, M. J., Mendez, G., Munoz, P., Mancera, L., Ruiz-Serrano, M. J., & Rodriguez-Sanchez, B. (2023). Identification of Mycobacterium abscessus Subspecies by MALDI-TOF Mass Spectrometry and Machine Learning. *J Clin Microbiol*, *61*(1), e0111022. https://doi.org/10.1128/jcm.01110-22

Ruijter, J. M., Barnewall, R. J., Marsh, I. B., Szentirmay, A. N., Quinn, J. C., van Houdt, R., Gunst, Q. D., & van den Hoff, M. J. (2021). Efficiency correction is required for accurate quantitative PCR analysis and reporting. *Clinical chemistry*, *67*(6), 829-842. https://doi.org/https://doi.org/10.1093/clinchem/hvab052

Ruijter, J. M., Ramakers, C., Hoogaars, W. M., Karlen, Y., Bakker, O., van den Hoff, M. J., & Moorman, A. F. (2009). Amplification efficiency: linking baseline and bias in the

analysis of quantitative PCR data. *Nucleic Acids Res*, *37*(6), e45. https://doi.org/10.1093/nar/gkp045

Ruiz-Villalba, A., van Pelt-Verkuil, E., Gunst, Q. D., Ruijter, J. M., & van den Hoff, M. J. (2017). Amplification of nonspecific products in quantitative polymerase chain reactions (qPCR). *Biomol Detect Quantif*, *14*, 7-18. https://doi.org/10.1016/j.bdq.2017.10.001

Sabin, A. P., Ferrieri, P., & Kline, S. (2017). Mycobacterium abscessus Complex Infections in Children: A Review. *Curr Infect Dis Rep*, *19*(11), 46. https://doi.org/10.1007/s11908-017-0597-2

Sahoo, R., Jadhav, S., & Nema, V. (2024). Journey of technological advancements in the detection of antimicrobial resistance. *J Formos Med Assoc*, *123*(4), 430-441. https://doi.org/10.1016/j.jfma.2023.08.008

Sam, I. K., Chen, Y. Y., Ma, J., Li, S. Y., Ying, R. Y., Li, L. X., Ji, P., Wang, S. J., Xu, J., Bao, Y. J., Zhao, G. P., Zheng, H. J., Wang, J., Sha, W., & Wang, Y. (2021). TB-QUICK: CRISPR-Cas12b-assisted rapid and sensitive detection of Mycobacterium tuberculosis. *J Infect*, *83*(1), 54-60. https://doi.org/10.1016/j.jinf.2021.04.032

Saukkonen, K., Lakkisto, P., Pettila, V., Varpula, M., Karlsson, S., Ruokonen, E., Pulkki, K., & Group, F. S. (2008). Cell-free plasma DNA as a predictor of outcome in severe sepsis and septic shock. *Clinical chemistry*, *54*(6), 1000-1007. https://doi.org/https://doi.org/10.1373/clinchem.2007.101030

Schrader, C., Schielke, A., Ellerbroek, L., & Johne, R. (2012). PCR inhibitors–occurrence, properties and removal. *Journal of applied microbiology*, *113*(5), 1014-1026.

Scientific, T. F. MagMAX™ Cell-Free DNA Isolation Kit. In.

Sedlackova, T., Repiska, G., Celec, P., Szemes, T., & Minarik, G. (2013). Fragmentation of DNA affects the accuracy of the DNA quantitation by the commonly used methods. *Biol Proced Online*, *15*(1), 5. https://doi.org/10.1186/1480-9222-15-5

Shallom, S. J., Gardina, P. J., Myers, T. G., Sebastian, Y., Conville, P., Calhoun, L. B., Tettelin, H., Olivier, K. N., Uzel, G., Sampaio, E. P., Holland, S. M., & Zelazny, A. M. (2013). New rapid scheme for distinguishing the subspecies of the Mycobacterium abscessus group and identifying Mycobacterium massiliense isolates with inducible clarithromycin resistance. *J Clin Microbiol*, *51*(9), 2943-2949. https://doi.org/10.1128/JCM.01132-13

Shallom, S. J., Moura, N. S., Olivier, K. N., Sampaio, E. P., Holland, S. M., & Zelazny, A. M. (2015). New Real-Time PCR Assays for Detection of Inducible and Acquired

Clarithromycin Resistance in the Mycobacterium abscessus Group. *J Clin Microbiol*, *53*(11), 3430-3437. https://doi.org/10.1128/JCM.01714-15

Shen, S. Y., Singhania, R., Fehringer, G., Chakravarthy, A., Roehrl, M. H. A., Chadwick, D., Zuzarte, P. C., Borgida, A., Wang, T. T., Li, T., Kis, O., Zhao, Z., Spreafico, A., Medina, T. D. S., Wang, Y., Roulois, D., Ettayebi, I., Chen, Z., Chow, S., . . . De Carvalho, D. D. (2018). Sensitive tumour detection and classification using plasma cell-free DNA methylomes. *Nature*, *563*(7732), 579-583. https://doi.org/10.1038/s41586-018-0703-0

Sin, D. D., Wu, L., & Man, S. F. (2005). The relationship between reduced lung function and cardiovascular mortality: a population-based study and a systematic review of the literature. *Chest*, *127*(6), 1952-1959. https://doi.org/10.1378/chest.127.6.1952

Singh, K., Kumari, R., Tripathi, R., Gupta, S., & Anupurba, S. (2020). Detection of clinically important non tuberculous mycobacteria (NTM) from pulmonary samples through one-step multiplex PCR assay. *BMC microbiology*, *20*, 1-6. https://doi.org/https://doi.org/10.1186/s12866-020-01952-y

Snyder, M. W., Kircher, M., Hill, A. J., Daza, R. M., & Shendure, J. (2016). Cell-free DNA comprises an in vivo nucleosome footprint that informs its tissues-of-origin. *Cell*, *164*(1), 57-68. https://doi.org/https://doi.org/10.1016/j.cell.2015.11.050

Soetaert, K., Subissi, L., Ceyssens, P. J., Vanfleteren, B., Chantrenne, M., Asikainen, T., Duysburgh, E., & Mathys, V. (2019). Strong increase of true and false positive mycobacterial cultures sent to the National Reference Centre in Belgium, 2007 to 2016. *Euro Surveill*, *24*(11), 1800205. https://doi.org/10.2807/1560-7917.ES.2019.24.11.1800205

Steindor, M., Hafkemeyer, S., Ruckes, C., Stehling, F., Naehrlich, L., & Ringshausen, F. C. (2023). Epidemiological trends in nontuberculous mycobacterial infection among people with cystic fibrosis in Germany. *International Journal of Infectious Diseases*, *129*, 32-39. https://www.ijidonline.com/article/S1201-9712(23)00036-X/pdf

Steindor, M., Nkwouano, V., Mayatepek, E., Mackenzie, C. R., Schramm, D., & Jacobsen, M. (2015). Rapid detection and immune characterization of Mycobacterium abscessus infection in cystic fibrosis patients. *PLoS One*, *10*(3), e0119737. https://doi.org/10.1371/journal.pone.0119737

Svec, D., Tichopad, A., Novosadova, V., Pfaffl, M. W., & Kubista, M. (2015). How good is a PCR efficiency estimate: Recommendations for precise and robust qPCR efficiency

assessments. *Biomolecular detection and quantification*, *3*, 9-16. https://doi.org/https://doi.org/10.1016/j.bdq.2015.01.005

Swango, K. L., Timken, M. D., Chong, M. D., & Buoncristiani, M. R. (2006). A quantitative PCR assay for the assessment of DNA degradation in forensic samples. *Forensic Sci Int*, *158*(1), 14-26. https://doi.org/10.1016/j.forsciint.2005.04.034

Tellinghuisen, J., & Spiess, A. N. (2014). Comparing real-time quantitative polymerase chain reaction analysis methods for precision, linearity, and accuracy of estimating amplification efficiency. *Anal Biochem*, *449*, 76-82. https://doi.org/10.1016/j.ab.2013.12.020

Terp, S. K., Pedersen, I. S., & Stoico, M. P. (2024). Extraction of Cell-Free DNA: Evaluation of Efficiency, Quantity, and Quality. *J Mol Diagn*, *26*(4), 310-319. https://doi.org/10.1016/j.jmoldx.2024.01.008

Thornton, B., & Basu, C. (2011). Real-time PCR (qPCR) primer design using free online software. *Biochem Mol Biol Educ*, *39*(2), 145-154. https://doi.org/10.1002/bmb.20461

Tippett, E., Ellis, S., Wilson, J., Kotsimbos, T., & Spelman, D. (2018). Mycobacterium abscessus complex: Natural history and treatment outcomes at a tertiary adult cystic fibrosis center. *Int J Mycobacteriol*, *7*(2), 109-116. https://doi.org/10.4103/ijmy.ijmy_55_18

Turcios, N. L. (2020). Cystic Fibrosis Lung Disease: An Overview. *Respir Care*, *65*(2), 233-251. https://doi.org/10.4187/respcare.06697

Ungerer, V., Bronkhorst, A. J., Uhlig, C., & Holdenrieder, S. (2022). Cell-Free DNA Fragmentation Patterns in a Cancer Cell Line. *Diagnostics (Basel)*, *12*(8), 1896. https://doi.org/10.3390/diagnostics12081896

Vallières, E., & Elborn, J. S. (2014). Cystic fibrosis gene mutations: evaluation and assessment of disease severity. *Advances in Genomics and Genetics*, 161-172.

Wang, L., Tian, W., Zhang, W., Wen, D., Yang, S., Wang, J., Han, X., Wang, J., Ding, W., Wang, L., Yu, Y., & Wu, W. (2024). A Machine learning model for predicting sepsis based on an optimized assay for microbial cell-free DNA sequencing. *Clin Chim Acta*, *559*, 119716. https://doi.org/10.1016/j.cca.2024.119716

Wang, W. (2015). The molecular detection of Corynespora Cassiicola on cucumber by PCR assay using DNAman software and NCBI. International conference on computer and computing technologies in agriculture,

Wilkens, H., Weingard, B., Lo Mauro, A., Schena, E., Pedotti, A., Sybrecht, G. W., & Aliverti, A. (2010). Breathing pattern and chest wall volumes during exercise in

patients with cystic fibrosis, pulmonary fibrosis and COPD before and after lung transplantation. *Thorax*, *65*(9), 808-814. https://doi.org/10.1136/thx.2009.131409

Wong, F. C., Sun, K., Jiang, P., Cheng, Y. K., Chan, K. C., Leung, T. Y., Chiu, R. W., & Lo, Y. M. (2016). Cell-free DNA in maternal plasma and serum: A comparison of quantity, quality and tissue origin using genomic and epigenomic approaches. *Clin Biochem*, *49*(18), 1379-1386. https://doi.org/10.1016/j.clinbiochem.2016.09.009

Xiao, G., He, X., Zhang, S., Liu, Y., Liang, Z., Liu, H., Zhang, J., Ou, M., Cai, S., Lai, W., Zhang, T., Ren, L., & Zhang, G. (2020). Cas12a/guide RNA-based platform for rapid and accurate identification of major Mycobacterium species. *Journal of clinical microbiology*, *58*(2), 10.1128/jcm. 01368-01319. https://doi.org/https://doi.org/10.1128/jcm.01368-19

Xue, X., Teare, M. D., Holen, I., Zhu, Y. M., & Woll, P. J. (2009). Optimizing the yield and utility of circulating cell-free DNA from plasma and serum. *Clin Chim Acta*, *404*(2), 100-104. https://doi.org/10.1016/j.cca.2009.02.018

Ye, J., Coulouris, G., Zaretskaya, I., Cutcutache, I., Rozen, S., & Madden, T. L. (2012). Primer-BLAST: a tool to design target-specific primers for polymerase chain reaction. *BMC bioinformatics*, *13*, 134. https://doi.org/10.1186/1471-2105-13-134

Zhang, M., Wang, P., Li, C., Segev, O., Wang, J., Wang, X., Yue, L., Jiang, X., Sheng, Y., Levy, A., Jiang, C., & Chen, F. (2023). Comparative genomic analysis reveals differential genomic characteristics and featured genes between rapid- and slow-growing non-tuberculous mycobacteria. *Front Microbiol*, *14*, 1243371. https://doi.org/10.3389/fmicb.2023.1243371

Zhou, Y., Mu, W., Zhang, J., Wen, S. W., & Pakhale, S. (2022). Global prevalence of non-tuberculous mycobacteria in adults with non-cystic fibrosis bronchiectasis 2006-2021: a systematic review and meta-analysis. *BMJ open*, *12*(8), e055672. https://doi.org/10.1136/bmjopen-2021-055672

Zolin, A., Bossi, A., Cirilli, N., Kashirskaya, N., & Padoan, R. (2018). Cystic Fibrosis Mortality in Childhood. Data from European Cystic Fibrosis Society Patient Registry. *Int J Environ Res Public Health*, *15*(9), 2020. https://doi.org/10.3390/ijerph15092020

Appendices

Appendix 1

Figure removed due to copyright restriction.

Figure A1 CRISPOR output table of candidate guide RNAs (gRNAs) targeting the 23S rRNA locus of Mycobacterium abscessus. The table compiles guide sequences with corresponding PAM sites, predicted efficiency scores (Doench 2016, Moreno-Mateos), specificity scores (MIT and CFD), and predicted off-target sites. Highlighted gRNAs were chosen based on high on-target efficiency, low off-target binding, and no predicted human genome interaction. The guides were used to guide the design of a CRISPR-Cas12a detection assay to enhance specificity in cfDNA-based MABC diagnostics.

Appendix 2

Figure removed due to copyright restriction.

Figure A2 CRISPOR off-target analysis of shortlisted CRISPR-Cas12a guide RNAs assessed against the human genome. The table compiles guide sequences with corresponding PAM sites, predicted efficiency scores (Doench 2016, Moreno-Mateos), specificity scores (MIT and CFD), and predicted off-target sites.

Appendix 3

Target: **fastaInput.fa**
Rank: **7**
Target sequence: **AGATGCTCGTTACGCGCGGCAGG**

Off-targets		
Location	Number of mismatches	Sequence (including mismatches)
NC_010397.1:1466450	0	AGATGCTCGTTACGCGCGGCAGG

Shen et al. 2018 predictions of repair profile – statistics	
Reference sequence	GCGAAATTGCACTACGAGTAAAGATGCTCGTTACGCGCGGCAGGACGAAAAGACCCCGGG<>ACCTTCACTATAGCTTGGTATTGGCGTTTGGTTCGGTT
Frameshift frequency	59.72
Precision score	0.45
Frame +0 frequency	40.28
Frame +1 frequency	40.47
Frame +2 frequency	19.25
1-bp ins frequency	10.17
Highest del frequency	24.09
Highest ins frequency	8.47
Highest outcome frequency	24.09
Microhomology deletion frequency	72.30
Microhomology-less deletion frequency	17.53

Figure A3 CHOPCHOP off-target analysis confirming the specificity of the selected gRNA. No off-target interactions were identified within the human genome, and repair profile statistics.

Appendix 4

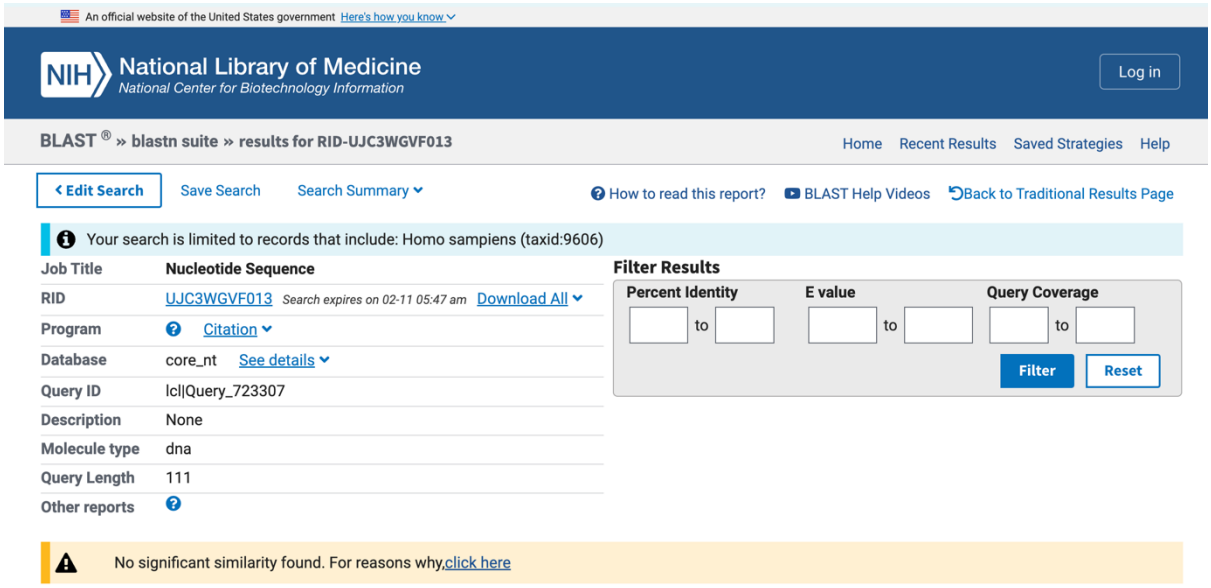

Figure A4 NCBI BLAST search of gRNA target sequence against Homo sapiens genome. The analysis shows no significant alignment of the 111 bp target region with any human DNA, ensuring high specificity for downstream CRISPR-Cas12a-based detection.